

## The Seasonal Cycle of Low Stratiform Clouds

STEPHEN A. KLEIN AND DENNIS L. HARTMANN

*Department of Atmospheric Sciences, University of Washington, Seattle, Washington*

(Manuscript received 21 August 1992, in final form 11 January 1993)

### ABSTRACT

The seasonal cycle of low stratiform clouds is studied using data from surface-based cloud climatologies. The impact of low clouds on the radiation budget is illustrated by comparison of data from the Earth Radiation Budget Experiment with the cloud climatologies. Ten regions of active stratocumulus convection are identified. These regions fall into four categories: subtropical marine, midlatitude marine, Arctic stratus, and Chinese stratus. With the exception of the Chinese region, all the regions with high amounts of stratus clouds are over the oceans.

In all regions except the Arctic, the season of maximum stratus corresponds to the season of greatest lower-troposphere static stability. Interannual variations in stratus cloud amount also are related to changes in static stability. A linear analysis indicates that a 6% increase in stratus fractional area coverage is associated with each 1°C increase in static stability. Over midlatitude oceans, sky-obscuring fog is a large component of the summertime stratus amount. The amount of fog appears to be related to warm advection across sharp gradients of SST.

### 1. Introduction

For many years it has been recognized that clouds strongly affect the earth's climate. Among the most important of these effects are the changes in radiative fluxes caused by clouds. Clouds enhance the albedo of the surface-atmosphere column by scattering solar radiation; furthermore, they emit less thermal radiation to space than the surface-atmosphere column would under clear-sky conditions. For low optically thick clouds, the albedo effect dominates, so that the net effect of these clouds on the earth's radiation budget is strongly negative (Manabe and Strickler 1964; Manabe and Wetherald 1967). Recent observational evidence indicates that low clouds reduce the net radiation balance on a global annually averaged basis by about  $15 \text{ W m}^{-2}$  (Hartmann et al. 1992).

Because of the sensitivity of the earth's radiation budget to low clouds, understanding what governs the abundance of low clouds is a crucial climate question (Randall et al. 1984). Some global climate models (GCMs) indicate that a 20% increase in the relative amount of low clouds could balance the greenhouse warming expected from a doubling of carbon dioxide (Slingo 1990). Yet different GCMs disagree about the magnitude and even the sign of the cloud feedback (Cess et al. 1989). Thus, with theories and models of fractional cloudiness still primitive, it would seem appropriate to ask, What is the current seasonal distribution of the low clouds and what causes seasonal and regional variations in low-cloud abundance?

Low stratiform clouds are primarily found over the earth's oceans. Previous study of the dynamical conditions under which low stratiform clouds exist has led to a simple three-type classification of stratiform clouds. First, on the east side of the oceanic subtropical highs, where the trade winds climatologically blow from mid-latitudes toward the intertropical convergence zone (ITCZ), stratocumulus clouds frequently occur. These clouds form over oceans with relatively cold sea surface temperatures (SSTs) and beneath a strong temperature inversion that caps the boundary layer. This trade inversion, thought to be maintained by subsidence in the descending branch of the Hadley circulation, limits the stratiform convection to the boundary layer, ensuring that the cloud remains low. As air in the trade winds approaches the ITCZ and warmer water, the trade inversion generally rises and weakens, and deeper cumulus convection replaces the stratiform clouds. How cumulus clouds supplant stratiform clouds is a question of active research. Subtropical stratocumulus clouds have been extensively studied, both by field experiments [e.g., FIRE, off the coast of California in the summer of 1987 (Albrecht et al. 1988), and ASTEX near the Azores in June 1992] and using a wide variety of models: simple mixed-layer models, large-eddy simulations, and GCMs (Lilly 1968; Moeng 1986; Randall et al. 1985; Schubert et al. 1979a).

Also among the known types of stratocumulus clouds are those that form in winter over the warm western boundary currents, for example, the Kuroshio and the Gulf Stream. When cold continental air blows

*Corresponding author address:* Stephen A. Klein, Department of Atmospheric Sciences, AK-40, University of Washington, Seattle, WA 98195.

over the warm currents, the resulting strong surface fluxes of heat and moisture rapidly deepen the boundary layer and convection begins. This driving of convection by strong surface fluxes is distinct from that of subtropical stratocumulus in which strong thermal radiative cooling at cloud top maintains convection. Despite this important difference, these clouds can be modeled using the same mixed-layer models that describe subtropical stratus (Schubert et al. 1979b).

Arctic stratus, a third type of low stratiform clouds, forms primarily in summer and in many cases results from radiative cooling of moist air that has entered the Arctic from subpolar latitudes (Curry et al. 1988; Herman and Goody 1976). Unique features of Arctic stratus include the tendency to form multiple cloud layers and the common occurrence of humidity inversions, that is, increases in humidity from beneath to above the inversion.

Other types of stratus not as widely recognized include the wintertime stratus found in the southeastern Chinese plain and the summertime stratus found over all midlatitude oceans between 45°N and 60°N.

In this analysis, we take results from a global analysis of cloud distributions (Warren et al. 1986; 1988) and define regions of climatologically common stratus. Furthermore, we will attempt to understand the seasonal cycle of stratus clouds in each region in terms of the large-scale dynamic (e.g., surface divergence) and thermodynamic (e.g., sea surface temperature, air-sea temperature difference, inversion strength) parameters upon which the clouds are thought to depend. Following a description of the data used in this study, the regions of active stratocumulus convection are defined from the surface-based climatology of low clouds. These regions are compared to the net cloud forcing as determined by the Earth Radiation Budget Experiment (Barkstrom 1984) to demonstrate how strongly stratus affects the net radiation budget. Section 4 discusses the seasonal variation in the marine subtropical stratus regions, while section 5 does the same for other stratus regions. In sections 6 and 7, some aspects of the interannual and interregional variation in stratus cloud amounts are discussed, and conclusions follow in section 8.

## 2. Data

The cloud data are taken from the climatological atlases of cloud properties recently published by Warren et al. (1986; 1988). The data used in both atlases are routine weather observations that were coded into the World Meteorological Organization's synoptic code (World Meteorological Organization 1974). Approximately 116 million land-based observations are analyzed for the period 1971–1981. For the ocean atlas, approximately 43 million ship (both commercial and military) observations are taken from the Comprehensive Ocean–Atmosphere Data Source (COADS)

(Woodruff et al. 1987). The period of analysis for the ocean atlas is December 1951 to November 1981.

The cloud information available in the synoptic code includes the amount of sky covered by clouds (in eighths of sky) as well as the amount of low clouds. Three levels (high, middle, and low) of clouds are distinguished, and the observer can specify the cloud type at each level with one of 27 codes (9 for each level). In addition, in reports of the present weather the observer may include information such as precipitation or fog present. For the cloud atlas analyses, low clouds are divided into three cloud types: cumulonimbus, cumulus, and stratus. Included in the definition of "stratus" are low clouds of slightly varying types: stratus, stratocumulus, fractocumulus, fractostratus, and sky-obscuring fog. For brevity, stratus in this paper will be understood to include the sum of all these cloud types. The amount of sky-obscuring fog is also reported separately in the atlases.

Cloud amounts are averaged seasonally and reported at a resolution of 5° latitude by 5° longitude between 50°N and 50°S with less longitudinal resolution poleward of 50° latitude. Cloud amounts, which represent the time average of the percent of sky covered by that cloud type at that level (high, middle, or low), are reported only if the sampling error is believed to be less than 3%. The minimum number of observations in a season necessary to reduce the sampling error below 3% is estimated to be 100 for ocean regions and 200 for land regions. The lower number for ocean regions reflects the smaller day-to-day and geographical variations in cloud amounts. For further information on biases and the method of analysis the reader is referred to the cloud atlases.

For comparison with the cloud atlas data, a monthly climatology of SST, air temperature, sea level pressure, and surface winds was constructed from the COADS monthly summaries for the same period as the ocean atlases, December 1951 to November 1981. Climatological averages were formed for every 2° latitude by 2° longitude box for which monthly averages were reported in at least 15 out of the 30 years. The climatological monthly mean winds were smoothed in space by two applications of a 1-2-1 filter on the 2° box averages to aid in the computation of divergences from surface winds.

For upper-air data, mapped analyses from the European Centre for Medium-Range Weather Forecasting (ECMWF) for the years 1980 through 1987 were averaged to provide a monthly climatology of 700-mb temperatures. The 700-mb level was chosen for upper-air data (as opposed to 850 mb) because as air flows equatorward the height of the inversion in the subtropics rises from about 900 mb far from the ITCZ to about 750 mb near the ITCZ (Neiburger et al. 1961; Riehl et al. 1951; Von Ficker 1936a; Von Ficker 1936b). The upper-air temperature climatology is combined with the surface air temperature climatology

to form a measure of the inversion strength, or static stability of the lower troposphere:

$$\Delta\theta \equiv \theta(p = 700 \text{ mb}) - \theta(p = \text{sea level pressure}, T = \text{surface air temperature}), \quad (1)$$

where  $\Delta\theta$  is the difference in potential temperature between 700 mb and the surface.

### 3. Net cloud forcing and regional definition

The Earth Radiation Budget Experiment (ERBE) has characterized the earth's radiation budget and the effects of clouds on the earth's radiation budget with unprecedented detail and accuracy (Barkstrom 1984; Barkstrom and Smith 1986). The primary goal of ERBE is to measure the amount of solar energy entering the earth's atmosphere, the amount reflected back to space, and the amount of thermal (or longwave) radiation emitted to space. Through the use of a scene identification algorithm, ERBE tries to identify which pixels correspond to clear skies and which correspond to cloudy skies. By comparison of the radiative fluxes from the clear-sky pixels with those of the cloudy-sky pixels, ERBE assesses the direct effect of clouds on the radiation budget (Harrison et al. 1990; Ramanathan et al. 1989). This direct effect is quantified by the definition of cloud forcing terms: shortwave cloud forcing, longwave cloud forcing, and net cloud forcing. If  $Q_{\text{clear}}$  is the average clear-sky reflected solar flux (in units of watts per square meter) and  $Q_{\text{average}}$  is the av-

erage reflected solar flux (from all pixels), then  $\Delta Q$ , the shortwave cloud forcing is defined as

$$\Delta Q \equiv Q_{\text{clear}} - Q_{\text{average}}, \quad (2)$$

where  $\Delta Q$  is a function of time and location on the earth. With this definition  $\Delta Q < 0$ , in general, as most clouds are more reflective than their underlying surfaces. Thus, the atmosphere-surface column loses energy that it might have kept in the absence of clouds. Similarly, if  $F_{\text{clear}}$  is the clear-sky thermal flux leaving the top of the atmosphere and  $F_{\text{average}}$  is the average thermal flux, the longwave cloud forcing,  $\Delta F$ , is

$$\Delta F \equiv F_{\text{clear}} - F_{\text{average}}. \quad (3)$$

In general,  $\Delta F > 0$ , as the tops of most clouds are colder than their underlying surfaces with the result that clouds reduce the amount of thermal radiation lost to space. Finally, the net cloud forcing is the sum of the longwave and shortwave cloud forcings:

$$\Delta R = \Delta F + \Delta Q. \quad (4)$$

On a global annually averaged basis, the shortwave cloud forcing is greater in magnitude than the longwave cloud forcing such that the "net effect" of clouds on the earth's top of the atmosphere radiation budget is to cool the planet approximately  $17 \text{ W m}^{-2}$  (Harrison et al. 1990). For low stratiform clouds we expect  $\Delta R < 0$ , as the shortwave cloud forcing of low stratiform clouds is much greater in magnitude than the longwave cloud forcing.

## Net Radiative Cloud Forcing

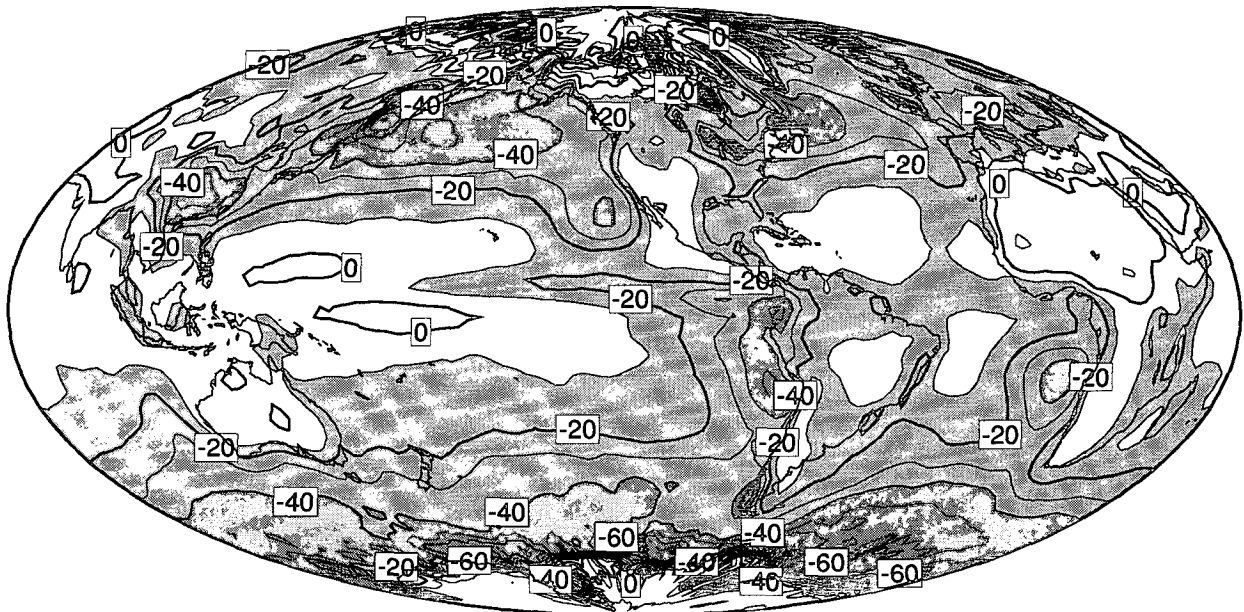
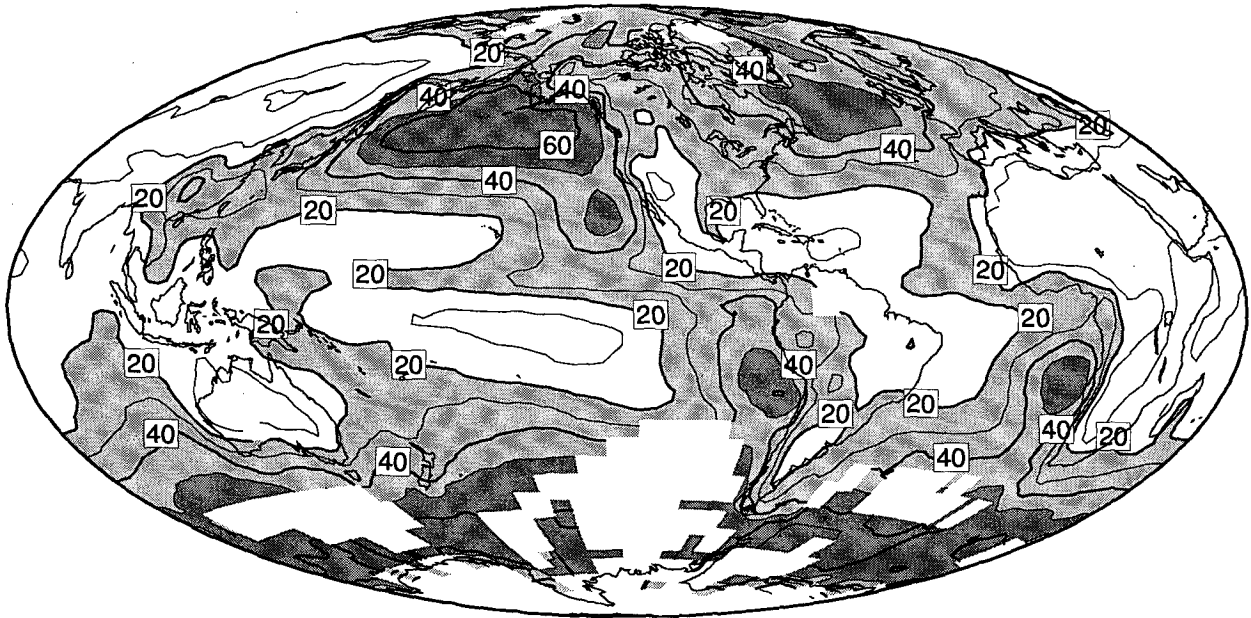


FIG. 1. Net radiative cloud forcing as seen by the Earth Radiation Budget Experiment (in  $\text{W m}^{-2}$ ) for February 1985 through January 1987. Contour interval is  $10 \text{ W m}^{-2}$ .

Figure 1 displays the global distribution of net cloud forcing averaged for the two years from February 1985 through January 1987. On this map, seven distinct regions of cloud forcing less than  $-40 \text{ W m}^{-2}$  exist. Three of these regions lie just to the west of the coasts of California, Peru, and Namibia; one over southeastern

China; another to the east of Labrador; and two extensive regions, one in the northern Pacific, and one that almost circles Antarctica in the Circumpolar Ocean. It is interesting to note that with the exception of southeastern China, all of the regions with strong negative cloud forcing occur over the ocean.

### Annual Stratus Cloud Amount



### JJA Stratus Cloud Amount

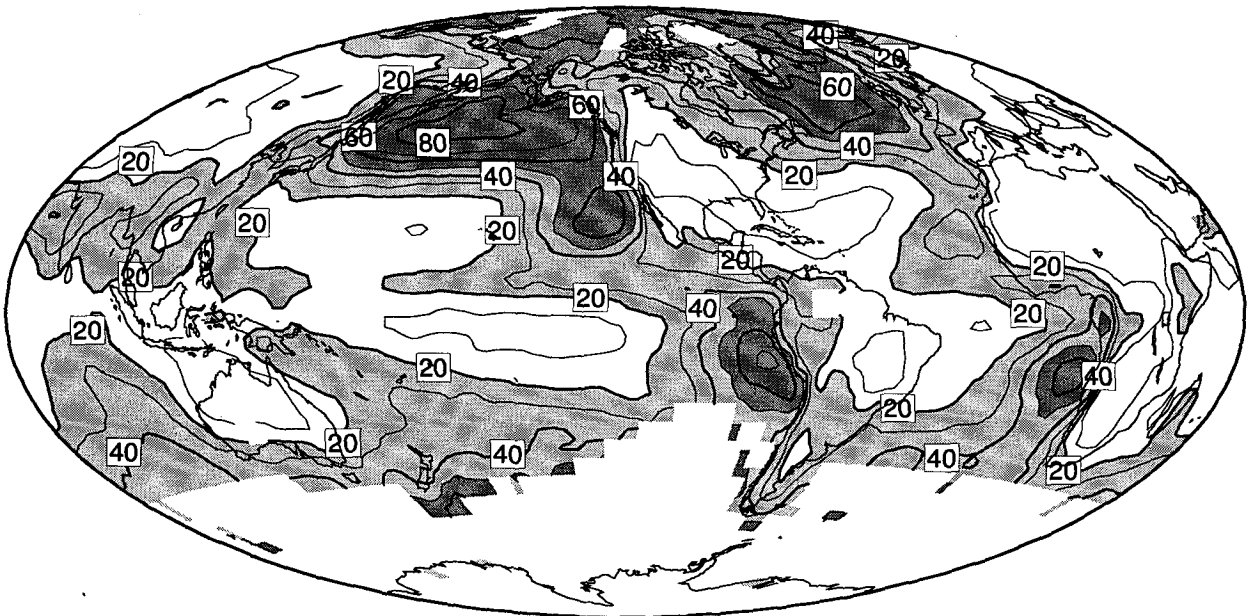


FIG. 2. The average stratus, stratocumulus, and sky-obscuring fog cloud amount in percent as seen by surface-based observers (a) annually; (b) for June, July, and August; and (c) for December, January, and February. Missing data indicates regions where fewer than 100 observations (for the ocean) or 200 observations (for land) have been recorded in a given season. Contour interval is 10%.

## DJF Stratus Cloud Amount

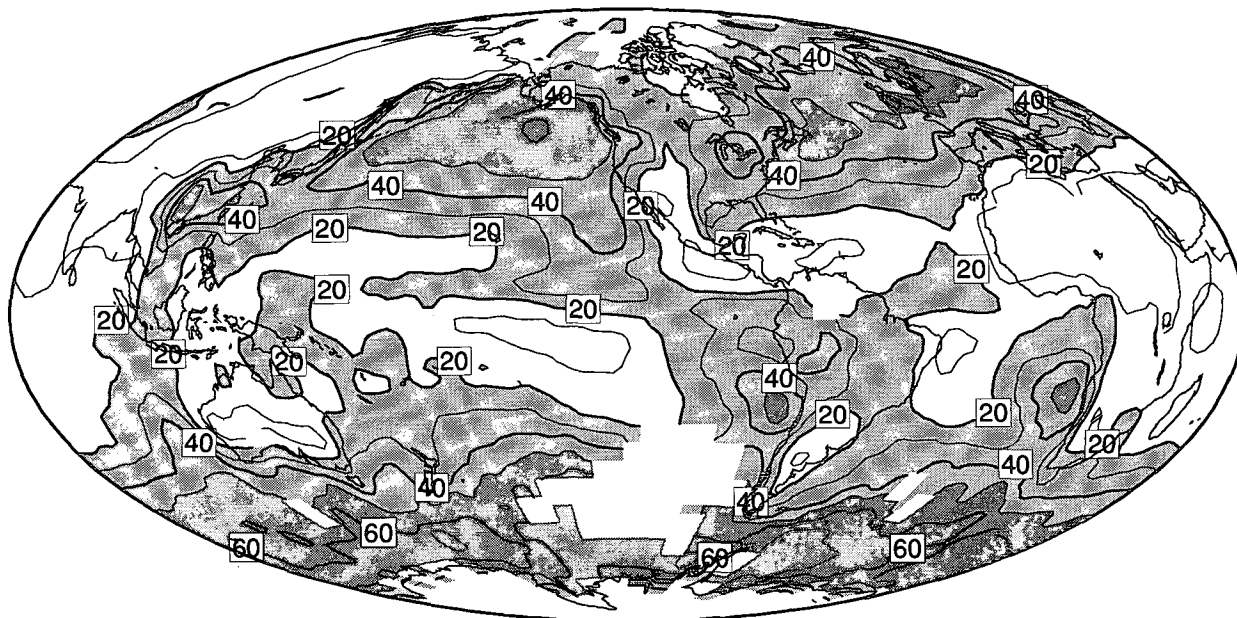


FIG. 2. (Continued)

Figure 2a displays the annually averaged stratus cloud amount from the Warren et al. (1986, 1988) atlases. Stratus clouds are primarily found in the marine environment as stratus cloud amounts average 17.5% over land but 34% over the ocean. The globally averaged stratus cloud amount is 29%. The greatest amounts of stratus occur on the east side of subtropical oceans and over the midlatitude and Arctic oceans. Minima in stratus amounts occur over the western parts of subtropical oceans (e.g., to the west of Hawaii) where small trade wind cumuli are the predominant cloud type. In June, July, and August (JJA), stratus amounts greater than 60% are seen in the subtropical oceans near California, Peru, and Namibia, and in the Arctic and the North Atlantic (Fig. 2b). In the North Pacific stratus amounts exceed 80%. During December, January, and February (DJF), high amounts of stratus are found in the Circumpolar Ocean, southeastern China, and the storm track regions of the North Pacific and the North Atlantic (Fig. 2c).

The relationship between the climatological amounts of stratus and the annual net cloud forcing is apparent (compare Fig. 1 with Fig. 2a): regions with climatologically high amounts of stratus are regions with strongly negative cloud forcing. Based on this comparison, ten stratus regions are defined (Table 1). The seasonal cycle of stratus clouds in each of these regions will be examined below.

The relationship between stratus clouds and net cloud forcing can be displayed entirely using satellite data. The International Satellite Cloud Climatology

Project (ISCCP) analyzed geosynchronous narrowband data to determine the space-time distribution of clouds. The C1 cloud product provides the amounts of various types of clouds every three hours as a function of location on earth. The cloud types are distinguished by cloud-top height and optical depth. Clouds with tops beneath 680 mb ( $\approx 3.3$  km) and optical depths greater than 3.55 (albedos greater than approximately 30%) are defined as "stratus" (Rossow and Schiffer 1991). This definition of "stratus" is obviously only approximate. Figure 3 is a scatterplot of the monthly averaged ISCCP stratus cloud fraction against the ERBE cloud forcing for the five marine subtropical stratus regions (Californian, Peruvian, Namibian, Canarian, and Australian) for the 12 months between March 1985 and February 1986. That the net cloud forcing and stratus cloud amounts are so well correlated indicates 1) few other clouds are present that would strongly influence the radiation budget in these regions and 2) the effects of variations (both annually and interregional) in other parameters (e.g., solar zenith angles, liquid water paths, and effective cloud-drop radii) on the net radiation balance are secondary (for the subtropical regions) to the direct effect of the amount of stratus present. Furthermore, stratus clouds affect the net radiation balance at the rate of approximately  $-1.00 \text{ W m}^{-2}$  per percent cloudiness in these regions. By considering low clouds of all optical thicknesses globally, Hartmann et al. (1992) found the sensitivity of the radiation balance to low clouds to be  $-0.63 \text{ W m}^{-2}$  per percent cloudiness.

TABLE 1. The ten stratus regions, their geographical extent, the season, and amount (%) of maximum stratiform cloudiness (DJF = December, January, and February, etc.), the month and value ( $^{\circ}\text{C}$ ) of maximum static stability, the season and amount (%) of minimum stratiform cloudiness, and the month and value ( $^{\circ}\text{C}$ ) of minimum static stability.

Region	Location	Season and amount (%) of maximum stratus	Month and value ( $^{\circ}\text{C}$ ) of maximum stability	Season and amount (%) of minimum stratus	Month and value ( $^{\circ}\text{C}$ ) of minimum stability
<i>Subtropical marine stratus</i>					
Peruvian <sup>a</sup>	10°–20°S, 80°–90°W	SON 72	Oct 22	DJF 42	Feb 18
Namibian	10°–20°S, 0°–10°E	SON 75	Sep 22	MAM 48	Feb 17
Californian	20°–30°N, 120°–130°W	JJA 67	Jun 22	DJF 45	Feb 18
Australian	25°–35°S, 95°–105°E	DJF 45	Feb 18	JJA 41	Jun 15
Canarian	15°–25°N, 25°–35°W	JJA 35	Jun 16	SON 17	Oct 13
<i>Midlatitude marine stratus</i>					
North Pacific	40°–50°N, 170°–180°E	JJA 82	Jul 21	DJF 54	Jan 8
North Atlantic	50°–60°N, 35°–45°W	JJA 68	Jul 20	DJF 51	Dec 10
Circumpolar Ocean <sup>a,b</sup>	50°–65°S	DJF? 62	Feb 15	? ?	Sep 13
Arctic <sup>a</sup>	80°–90°N	JJA 62	Jan 28	DJF 18	Aug 20
China <sup>a</sup>	20°–30°N, 105°–120°E	DJF 51	Feb 19	JJA 24	Aug 13

<sup>a</sup> In the computation of static stability (1), ECMWF climatological 1000-mb temperatures replace COADS surface air temperatures.

<sup>b</sup> In the Circumpolar Ocean, there are few ship reports during austral winter; thus the annual cycle of stratus clouds is uncertain.

#### 4. Marine subtropical stratus

In this section, the seasonal variation of stratus cloud amounts in the five marine subtropical regions (Table 1) is compared with the annual variation in dynamic and thermodynamic parameters that are thought to influence the occurrence of stratus. The seasonal cycle of these clouds in all ten regions is displayed in Fig. 4.

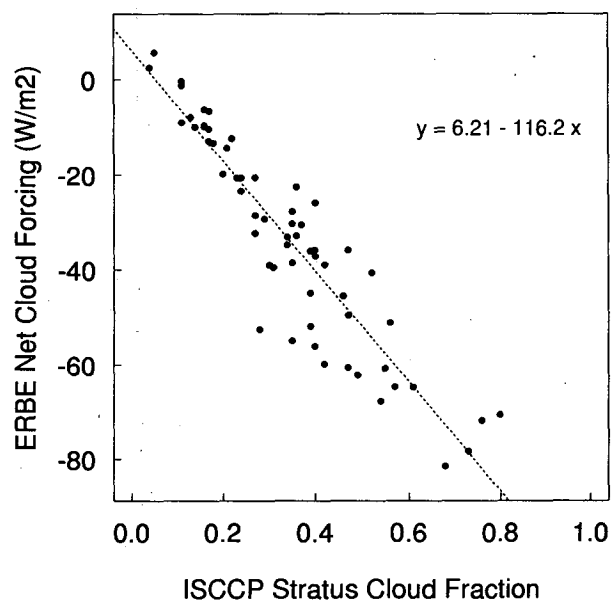


FIG. 3. Scatterplot of monthly ERBE net cloud forcings (in  $\text{W m}^{-2}$ ) against ISCCP stratus cloud fractions for the five subtropical stratus regions defined in Table 1 for the year March 1985 through February 1986. A least-squares regression line is plotted.

Stratus off the coast of California has been studied more frequently than stratus in any other region. In the Californian region, the summertime conditions under which stratus seem to occur include a well-developed subtropical high, equatorward-blowing trade winds whose divergence is an indication of strong subsidence aloft, and a sharp temperature inversion at the top of a well-mixed layer of typical depth 1000 m.

For all of these regions we find that the seasonal cycle of stratus cloud amount is closely tied to the seasonal cycle of static stability, and not directly related to the seasonal cycles of other parameters such as divergence or the strength of the subtropical high.

##### a. Californian stratus

Figure 5 displays the monthly climatologies of these parameters averaged over the Californian stratus region. The air temperature closely tracks the SST, with the air temperature between  $0.5^{\circ}$  and  $1^{\circ}\text{C}$  cooler than the SST (Fig. 5a). With this sea–air temperature difference, climatologically weak surface fluxes of sensible heat alone could not be responsible for the maintenance of stratus clouds; rather, it is the strong cloud-top radiative cooling that is responsible for sustaining convection (Lilly 1968). Because 700-mb climatological temperatures have a wider range than surface temperatures, the annual cycle in static stability (1) parallels that of the 700-mb temperature (Fig. 5b). Stratus cloud amounts peak during JJA (the same season as the peak static stability) at around 67% while the minimum stratus occurs in DJF at around 45% (Fig. 5b). Divergences of surface winds are typically  $3 \times 10^{-6} \text{ s}^{-1}$ , with no measurable seasonal cycle (Fig. 5c). The seasonal

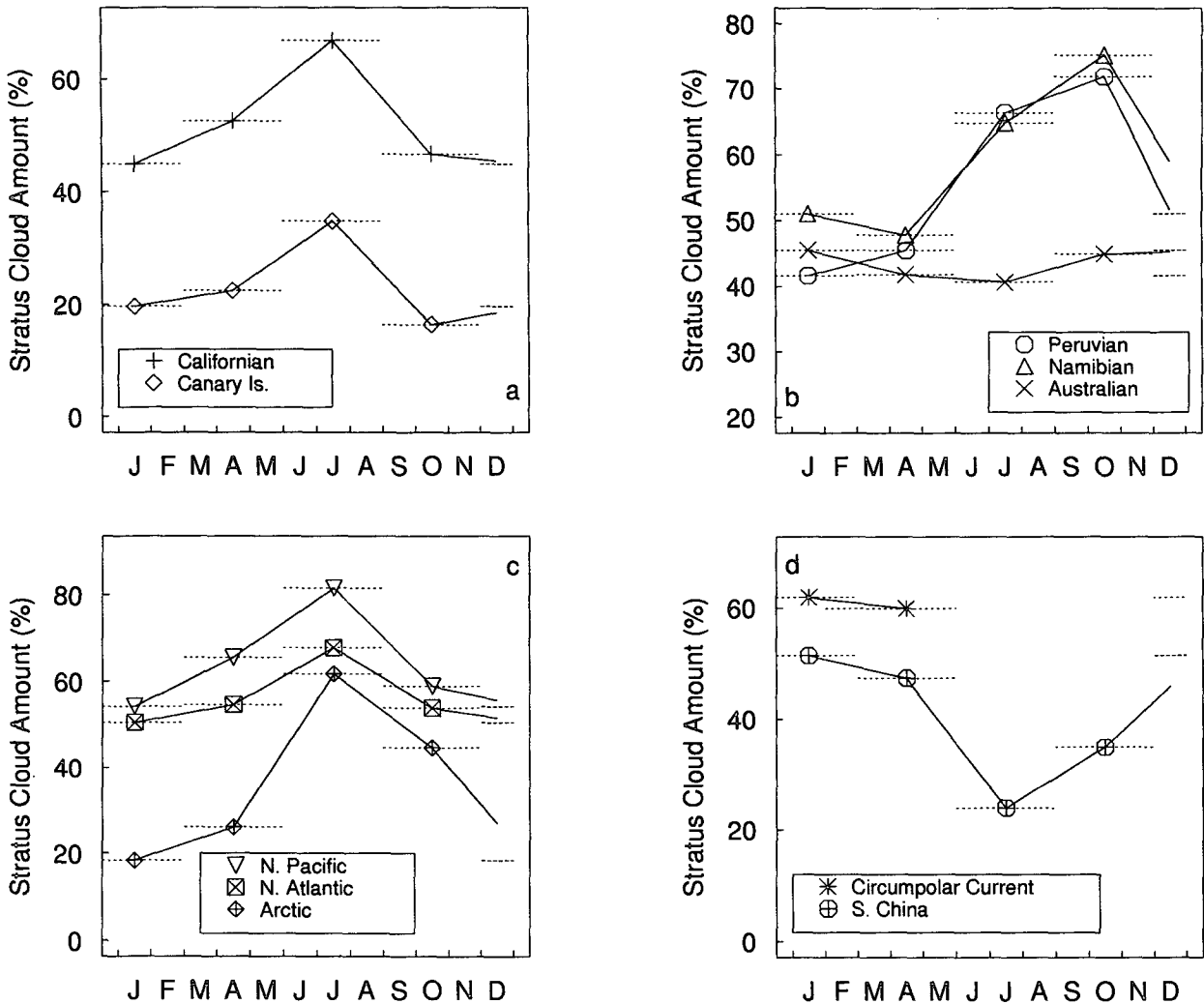


FIG. 4. Seasonally averaged stratus, stratocumulus, and sky-obscuring fog cloud amounts for (a) the Californian and Canarian stratus region; (b) the Peruvian, Namibian, and Australian stratus regions; (c) the North Pacific, North Atlantic, and Arctic Ocean; and (d) the Circumpolar Current region and southeast China. Horizontal dashed lines are drawn to indicate that cloud amounts are seasonally averaged. There is not enough data to establish an average cloud amount for the Circumpolar region for the June, July, and August season and for the September, October, and November season.

cycle of the strength of the subtropical high of the North Pacific (strongest in July and weakest in October) parallels that of the stratus cloud amount (Fig. 5c). Cloud forcings from the ERBE two-year average show that the minimum net cloud forcing occurs in July at  $-70 \text{ W m}^{-2}$ , the same month as the minimum longwave cloud forcing (Fig. 5d).

*b. Namibian stratus*

In contrast to the Californian stratus region, the range of SST in this Southern Hemisphere stratus region is greater than the range of 700-mb temperatures (Fig. 6a). Consequently, the static stability inversely follows the SST with maximum stability in September and October (Fig. 6b). Stratus cloud amounts in this

region peak in the SON season, the season of maximum stability, at nearly 75%. The months during which the subtropical high reaches its peak sea level pressure are July and August, somewhat earlier than the months of maximum cloudiness (Fig. 6c). Earth Radiation Budget Experiment cloud forcings show that the strongest net cloud forcing occurs during the months of August through November (Fig. 6d).

*c. Canarian stratus*

Although the seasonal cycle of stratus in the Canarian stratus region is similar to that of the Californian region, the Canary Island region has far less stratus (Fig. 4a). With regard to the thermodynamic parameters (figures not shown), SSTs are about  $3^{\circ}\text{--}5^{\circ}\text{C}$

## Californian Stratus Region

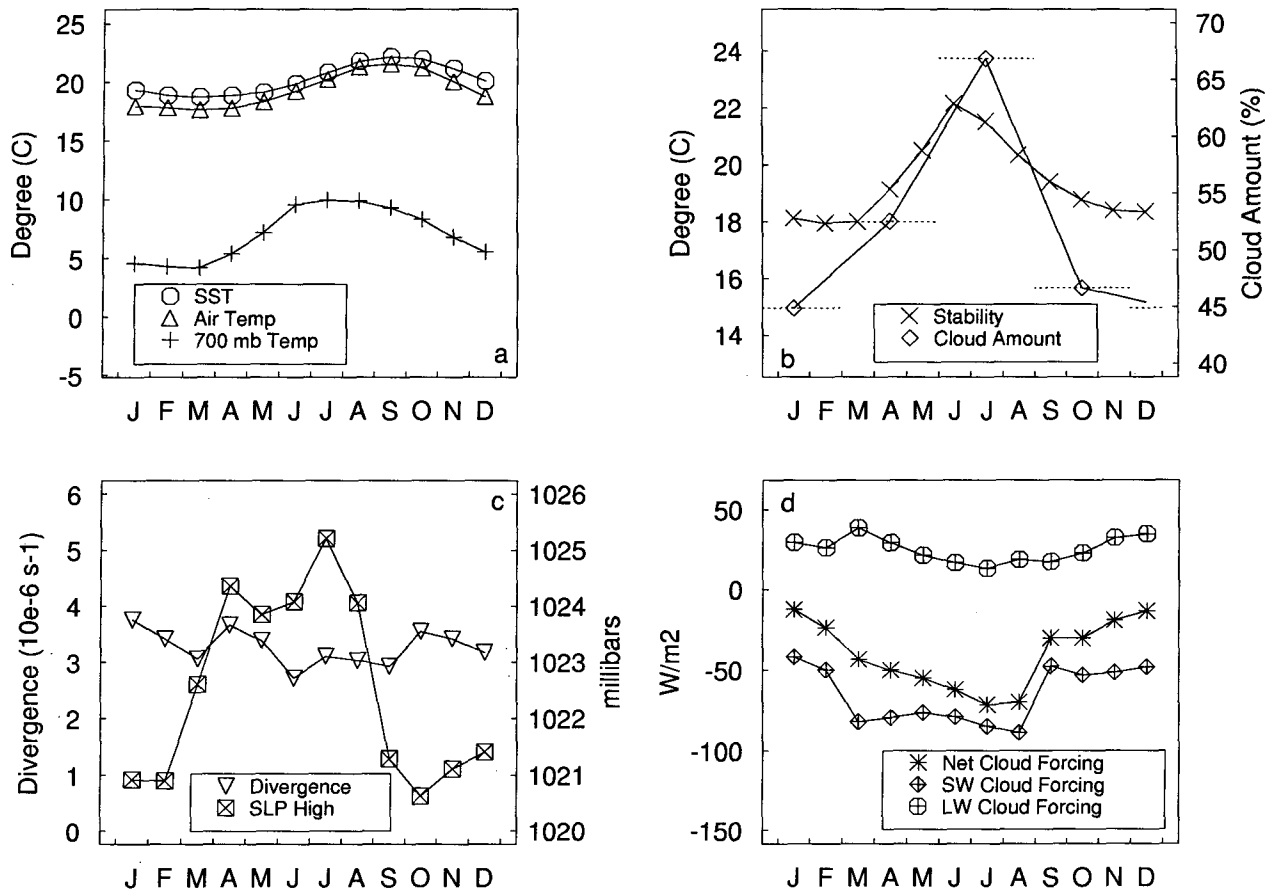


FIG. 5. The annual cycle of cloud, thermodynamic, and dynamic properties for the Californian stratus region (20°–30°N, 120°–130°W): (a) the sea surface, surface air, and 700-mb temperature; (b) the lower-tropospheric stability [ $\theta(700 \text{ mb}) - \theta(\text{sea level pressure})$ ], and stratus cloud amount (horizontal dashed lines are again drawn on the cloud amount data to remind the reader that cloud amount is seasonally averaged); (c) large-scale scale divergence of surface winds and the peak surface pressure of the subtropical high of the North Pacific ocean; and (d) shortwave, longwave, and net cloud forcings from the two-year ERBE climatology (in  $\text{W m}^{-2}$ ).

warmer in all seasons, while the 700-mb temperatures are very close to those in the Californian region. The annual range in 700-mb temperatures is still greater than that of the SSTs; consequently, the static stability is greatest in June or July (the season of maximum stratus) and lowest in October. With the warmer SSTs, the static stability in June is only about 16°C, about 6°C lower than the static stability in the Californian region in June. Lower stratus cloud amounts are apparently associated with lower values of the static stability. The minimum net cloud forcing for the ERBE two-year average occurs in July at nearly  $-30 \text{ W m}^{-2}$ , about one-half of the net cloud forcing for the same month in the Californian region.

### d. Australian stratus

In the Australian subtropical stratus region, the stratus cloud amount remains nearly constant throughout

the year, with a minimum of 40% in JJA and a maximum of 45% in DJF (Fig. 4b). The range in 700-mb temperatures (not shown) is slightly greater than that of the surface air temperatures; consequently, the static stability has a relatively small annual cycle with the peak stability of 18°C occurring in February (again the season of maximum stratus) and the minimum stability of 15°C occurring in June. In the southern Indian Ocean, the Mascarin high is strongest during the JJA season (the Indian monsoon season) with a peak sea level pressure of 1026 mb, while the minimum peak sea level pressure of 1019 mb occurs in January. Thus, the strength of the subtropical high in this region apparently does not determine the amount of stratus.

### e. Peruvian stratus

In the Peruvian stratus region, the peak stratus cloud amount occurs in SON at nearly 72%, with the mini-

### Namibian Stratus Region

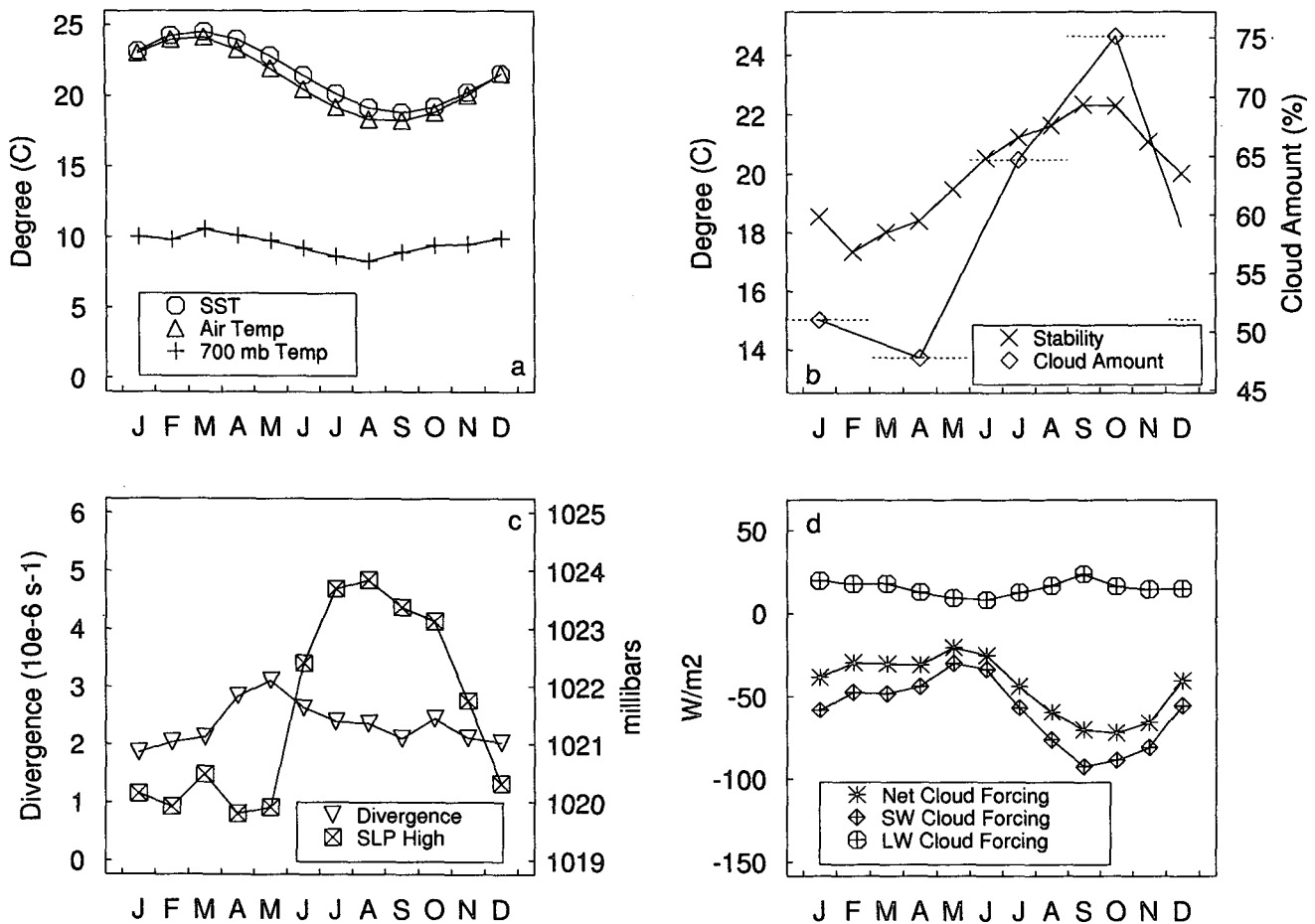


FIG. 6. As in Fig. 5 but for the Namibian stratus region (10°–20°S, 0°–10°E).

imum in DJF at 42% (Fig. 4b). The minimum SSTs occur in September and October at nearly 18°C. Because the 700-mb temperatures vary within a small range, the stability variations are dominated by SST changes and the maximum stability of about 22°C occurs during the SON season. Due to the paucity of observations in this region, the seasonal cycle in other parameters could not be determined.

Closer to the equator, it is interesting to analyze the variation in stratus cloud amounts near the equatorial cold tongue. Figure 7 presents stratus cloud amounts and thermodynamic and dynamic parameters averaged over longitude from 90°W to 110°W and over time from June through November. In the region from 10°S to 10°N winds climatologically blow from south to north with very small mean zonal motion. The amount of stratus clouds decreases toward the north and reaches a minimum near 2°S. Farther north, stratus clouds increase again and reach a maximum near 2.5°N and then decrease as the winds approach the ITCZ (near

8°N) (Fig. 7a). The Warren et al. cloud data with coarser resolution (5° latitude–longitude boxes) do not show this feature as strongly as the ISCCP cloud data (at 2.5° latitude–longitude resolution) for June through November 1985, a cold SST year. This feature can also be inferred in the net cloud forcing from ERBE (Fig. 1), as well as in the contoured stratus cloud amount for JJA (Fig. 2b).

It is possible to interpret the changes in stratus cloud amount in terms of the changes in the thermodynamic and dynamic properties of air following a trajectory through this region. As air blows northward toward the cold tongue and down the pressure gradient, the sea–air temperature difference reaches 0°C with the result that the surface flux of heat decreases (Fig. 7b). Data from the cruise of the *Discoverer* in October 1989 at 110°W showed that only at the equator were upward surface heat fluxes less than zero (Bond 1992). Furthermore, the divergence decreases to near zero by 5°S (Fig. 7c). Subtropical stratus clouds are generally most

## Equatorial Eastern Pacific Stratus Region

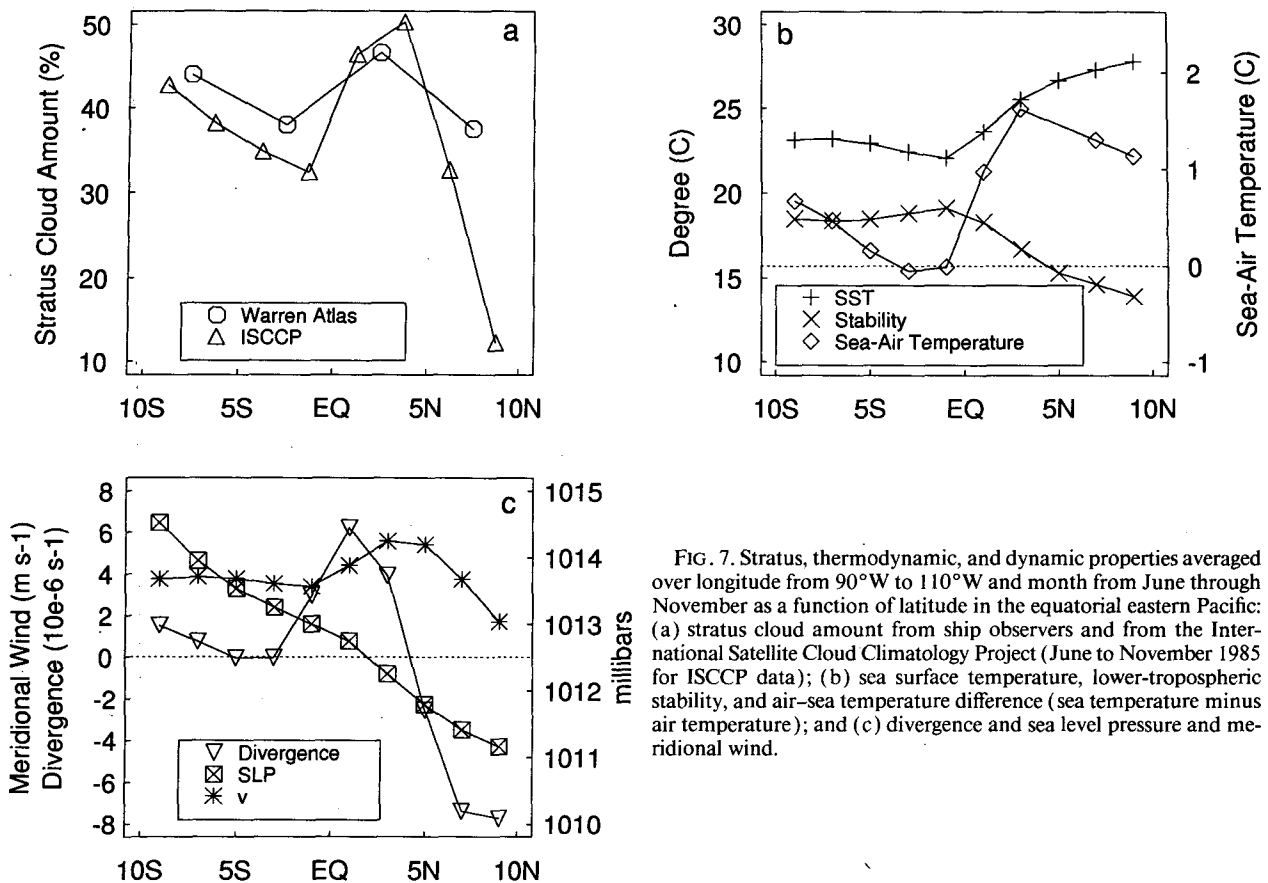


FIG. 7. Stratus, thermodynamic, and dynamic properties averaged over longitude from 90°W to 110°W and month from June through November as a function of latitude in the equatorial eastern Pacific: (a) stratus cloud amount from ship observers and from the International Satellite Cloud Climatology Project (June to November 1985 for ISCCP data); (b) sea surface temperature, lower-tropospheric stability, and air-sea temperature difference (sea temperature minus air temperature); and (c) divergence and sea level pressure and meridional wind.

frequent in conditions of steady divergence (with typical values of  $2 \times 10^{-6} \text{ s}^{-1}$ ) and steady surface fluxes characterized by a temperature difference of typically  $0.5^\circ\text{C}$ . Thus, the conditions of little mean divergence and very small surface fluxes that air encounters between  $5^\circ\text{S}$  and  $1^\circ\text{S}$  are unfavorable for the development of stratus clouds. The *Discoverer* also found the boundary layer to be the most stably stratified at  $1^\circ\text{S}$ , suggesting that turbulence (which would be necessary for stratus clouds) would be suppressed. Farther to the north ( $1^\circ\text{--}5^\circ\text{N}$ ), the surface air encounters substantially warmer SST. Consequently the sea-air temperature difference rises to  $1.5^\circ\text{C}$  resulting in strong surface fluxes of heat and moisture (at  $5^\circ\text{N}$  *Discoverer* heat fluxes reached  $50\text{--}80 \text{ W m}^{-2}$ ). Under conditions of fairly strong mean subsidence, this would lead to the production of stratus clouds. Indeed, it has been suggested that the stratus clouds that form as airstreams north from the cold tongue are similar to the stratus that form in the "cold air outbreaks" over the warm western boundary currents of the Northern Hemisphere (Deser and Wallace 1990). As air reaches the

ITCZ, the static stability decreases, deep convection takes place, and strong divergence is replaced by strong convergence. These conditions are clearly unfavorable for the production of low stratocumulus clouds capped by an inversion. The stratus cloud fraction in the ISCCP cloud data decreases from 50% at  $3.75^\circ\text{N}$  to 10% at  $8.75^\circ\text{N}$  (Fig. 7a). Although some of this decrease may be due to the increase of high clouds that block the view from space of low stratus clouds in the ITCZ, the Warren et al. cloud data (based on ship observers) also indicates a decrease in stratus clouds.

### 5. Midlatitude, Arctic, and Chinese stratus

Stratus cloud properties outside of the subtropics have been studied less frequently. In particular, the substantial amount of summertime stratus over midlatitude oceans (Fig. 2b) has rarely been noted. This would seem surprising given that there is as much stratus in these regions during the summer as there is in the subtropical stratus regions. In this section, we dis-

cuss the annual cycles of stratus clouds in the five extratropical stratus regions.

*a. North Pacific stratus*

In the North Pacific, the stratus cloud fraction reaches values of above 80% during JJA (Fig. 8b). In the wintertime, stratus clouds are also common with coverage above 50%. As in the Californian stratus region, the air at 700 mb undergoes a wider variation in temperature than that of the sea surface (Fig. 8a). With this wide swing in upper-air temperatures the stability varies from a minimum of 6°C in January to a maximum of 21°C in July, again the season of maximum stratus (Fig. 8b). This region also undergoes a strong cycle in the sea-air temperature difference with the air warmer than the sea by about 1°C in July and the sea warmer than the air by nearly 2°C during DJF (Fig. 8c). The surface divergence is very small in all seasons with a tendency for very weak divergence (compared

with the subtropical stratus regions) during the equinoctial seasons and very weak convergence during the winter season. From the perspective of ERBE, the longwave cloud forcing is constant at about  $40 \text{ W m}^{-2}$  while the shortwave and net cloud forcings have a very strong summertime minimum at  $-150 \text{ W m}^{-2}$  and  $-110 \text{ W m}^{-2}$ , respectively (Fig. 8d). Certainly much of this annual cycle in shortwave cloud forcing is caused by the greatly varying insolation and not changes in cloud amount or properties. However, it is striking that the shortwave cloud forcing is much greater than the Californian region's shortwave cloud forcing during JJA when the amounts of daily solar radiation reaching both regions are comparable (compare Fig. 8d with Fig. 5d).

With values of static stability of near 20°C in the summer season, it would be reasonable to ask, Is there a temperature inversion at the top of the cloud boundary layer in analogy to the trade wind inversion? Data from weather ships in the North Pacific (ship P) and

North Pacific Stratus Region

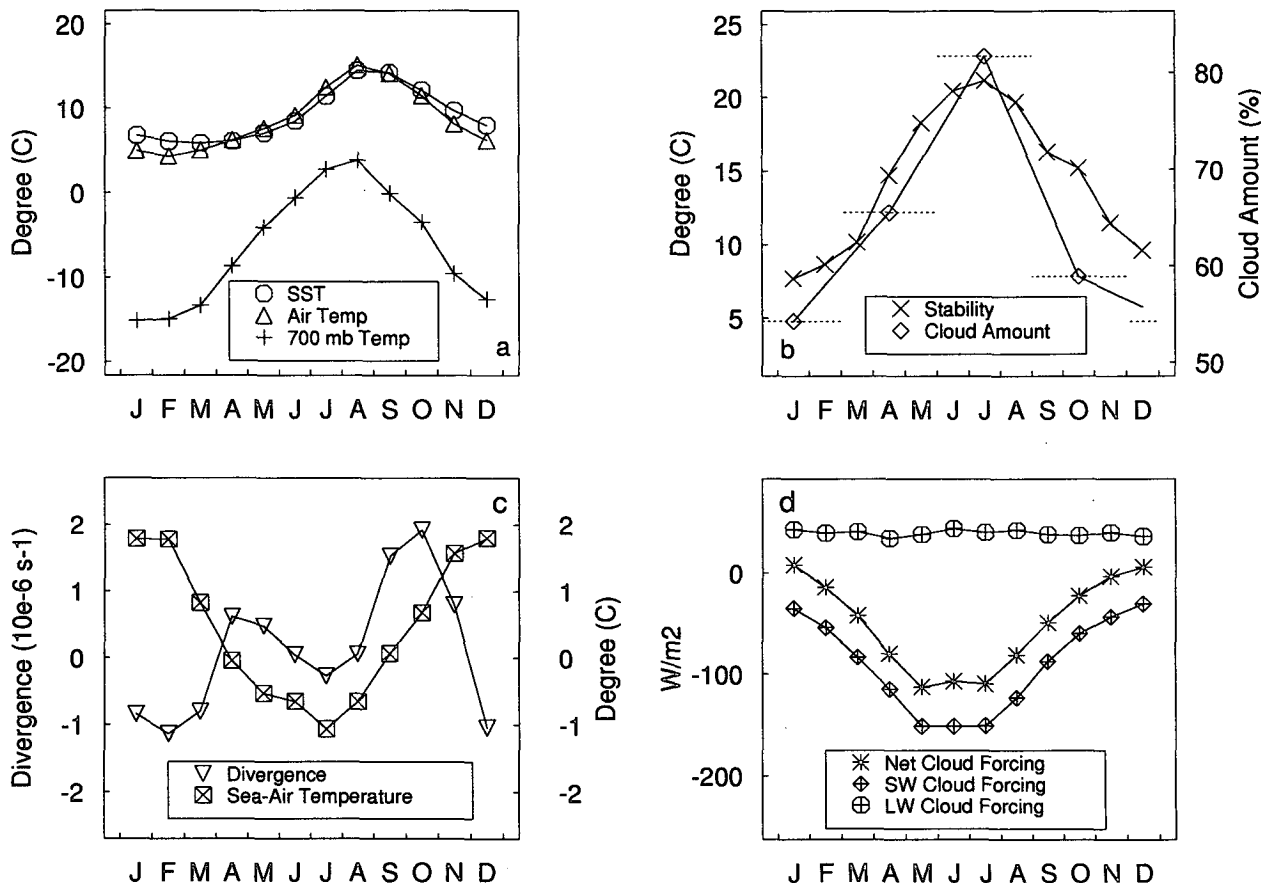


FIG. 8. As in Fig. 5 but for the North Pacific stratus region (40°–50°N, 170°–180°E).

North Atlantic (another region of high summertime values of stratus) (ships B and C) indicate that low-level inversions are frequent during the summertime (Fig. 9). At weather ship P (50°N, 145°W, substantially to the east of the maximum stratus region in the North Pacific), inversions at levels lower than 500 mb occur in at least 50% of the July soundings. Of the 17 000 soundings recorded at weathership B (57°N, 51°W, slightly west of the North Atlantic stratus region), 70% of the July soundings have inversions lower than 500 mb while only 29% of January soundings have inversions. Most of the summertime inversions lie quite low in the atmosphere. The mean July inversion base at ship B is at 947 mb while the mean inversion top is at 899 mb. The mean summertime sounding at ship B (Fig. 10) shows a surface inversion up to 950 mb with a mean 1000-mb relative humidity of 85%. What causes the low-level summer inversions over the North Atlantic and North Pacific? During summer the continents are substantially warmer than the surrounding oceans and a monsoonlike circulation develops with rising motion over the warm continents (and the resulting cumulus convection on land) and mean sinking motion over the colder oceans (resulting in low-level temperature inversions). This circulation is also associated with the strengthening and northward movement of the North Atlantic and North Pacific subtropical highs and the relative low surface pressures found over the Eurasian and North American continents during summer.

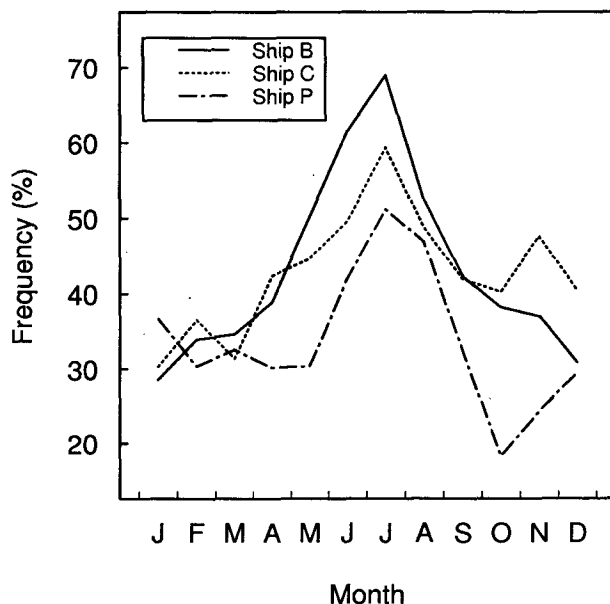


FIG. 9. The frequency of inversions lower than 500 mb at weather ships B (57°N, 51°W, 1949–1974), C (53°N, 35°W, 1949–1974), and P (50°N, 145°W, 1946–1970). The minimum inversion strength required to detect an inversion is 0.5°C.

In the wintertime, the strongly convective situation (with the surface air temperature substantially cooler than the sea, and weak lower-tropospheric stability) would suggest that the stratus clouds in this season result from “cold air outbreaks,” cold air masses behind cold fronts streaming over warmer ocean surfaces. In this strongly convective situation, the top of the boundary layer can be expected to be much higher than that found in the summer season. Of the 29% of January soundings with inversions at ship B, the mean inversion base is at 826 mb and the mean inversion top is at 781 mb, much higher than the summertime inversions. The mean January sounding from ship B shows that the mean lapse rate near the surface is nearly adiabatic while the cloud layer (indicated by the maximum in relative humidity) lies near 900 mb (Fig. 10).

One distinct difference between the subtropical and midlatitude stratus regions is the high abundance of fog observed in the latter regions. Figure 11a displays the frequency of occurrence of sky-obscuring fog over the Northern Hemisphere during JJA. Fog frequently occurs on the west side of the North Pacific and North Atlantic and in the Arctic basin where the ocean is ice free. During austral summer, sky-obscuring fog occurs more than 10% of the time over much of the Circumpolar Ocean with generally more fog in the western hemisphere and nearly 20% fog to the north of the Weddell Sea (Fig. 11b). What is the origin of this fog? One possible explanation is that under stable conditions [surface air temperatures warmer than sea temperatures (Fig. 8c)], moist air can cool to saturation by heat transfer to the ocean or (in the absence of clouds above) by longwave emission from air to space. Indeed, the annual cycle of fog parallels that of the sea–air temperature difference. For the region used to calculate averages in Fig. 8 (40°–50°N, 170E°–180°), sky-obscuring fog occurs 23% of the time during JJA, when the surface air is 1°C warmer than the SST, but only 1.33% during DJF when the air temperatures are nearly 2°C cooler than the ocean. What dynamic reasons may be responsible for maintaining summertime surface air warmer than the underlying ocean? When the subtropical high is well developed, surface air on the backside of the high blows northward from warm water to cold water (Fig. 12b). One would expect that surface air temperatures, which take a finite time to equilibrate with the ocean below, would be warmer than ocean temperatures where winds blown down the gradient in SST. Most of the fog is seen to occur west of 150°W, where this condition is met. The greatest amount of fog occurs over the Kurile Islands (>40%) where SSTs reach a local minimum less than 8°C (Fig. 12a). On the eastern side of the ocean, fog occurs mainly near the Oregon coast where winds climatologically blow toward cooler water (kept cool by coastal upwelling). On the Oregon coast, the climatological air temperature is 1°C warmer than the SST during JJA. The absence of fog, in the center of the subtropical stratus regions,

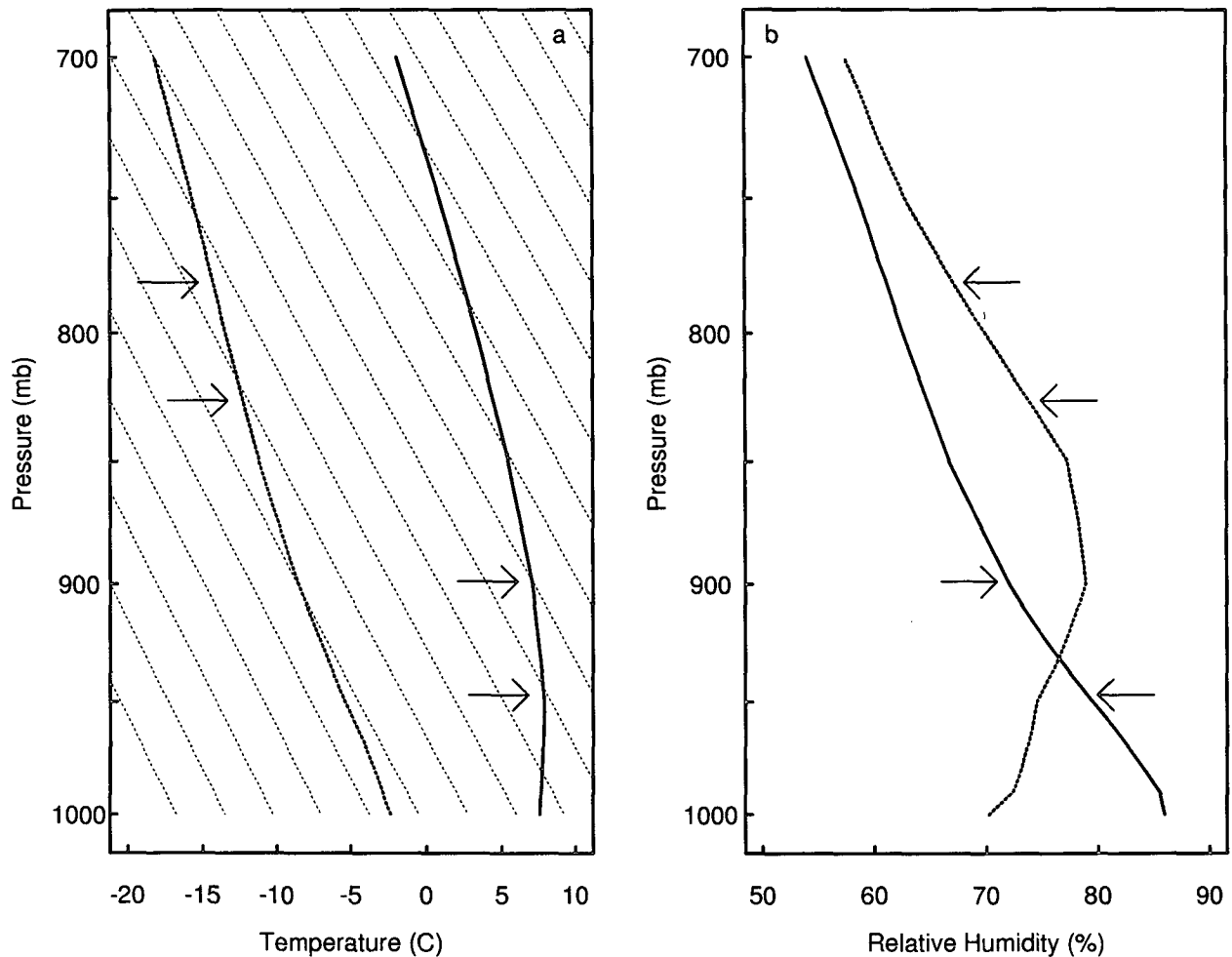


FIG. 10. Mean January and July soundings at weather ship B: (a) temperature and (b) humidity. The solid line indicates the July sounding, while the thick dashed line indicates the January sounding. Arrows indicate the mean pressure of the inversion base and inversion top for each month. Light dashed lines in panel (a) indicate adiabats.

where fog amounts are less than 0.5%, would seem to be because the climatological trade wind flow is up the gradient of SST, preventing surface air temperatures from rising above the SSTs below.

#### b. North Atlantic stratus

In general, the seasonal variation in cloud properties and the relevant thermodynamic and dynamic properties in the North Atlantic are similar to those in the North Pacific (figures not shown). Stratus peaks at 68% in JJA, the same season as the maximum stability. Fog occurs 10% of the time in JJA when the surface air is warmer than the SST. Cloud forcings from ERBE reveal a nearly constant value of longwave cloud forcing of around  $40 \text{ W m}^{-2}$  with a strong minimum in net forcing in July at  $-120 \text{ W m}^{-2}$ .

In the North Atlantic, fog is associated with gradients in SST (Figs. 12c,d). Over the western part of this

ocean, SSTs fall from nearly  $23^\circ\text{C}$  at  $40^\circ\text{N}$  to nearly  $9^\circ\text{C}$  just east of Newfoundland at  $48^\circ\text{N}$ . With winds blowing across the Gulf Stream toward the cold water near Newfoundland, a substantial amount of fog results. Indeed, during JJA, the surface air temperature is  $1^\circ\text{C}$  warmer than the SST near Newfoundland.

#### c. Circumpolar Ocean stratus

During the austral summer and fall stratus cloud amounts in the Circumpolar Ocean are nearly 60% with fog amounts in both season averaging 6% (Fig. 4d). There is not enough data to establish cloud amounts during austral winter and spring, the season of maximum ice extent when few ships are present. Data from the islands in this ocean have differing values of stratus amounts for these seasons, but it seems likely that the stratus amount is at least 40% during austral winter and spring.

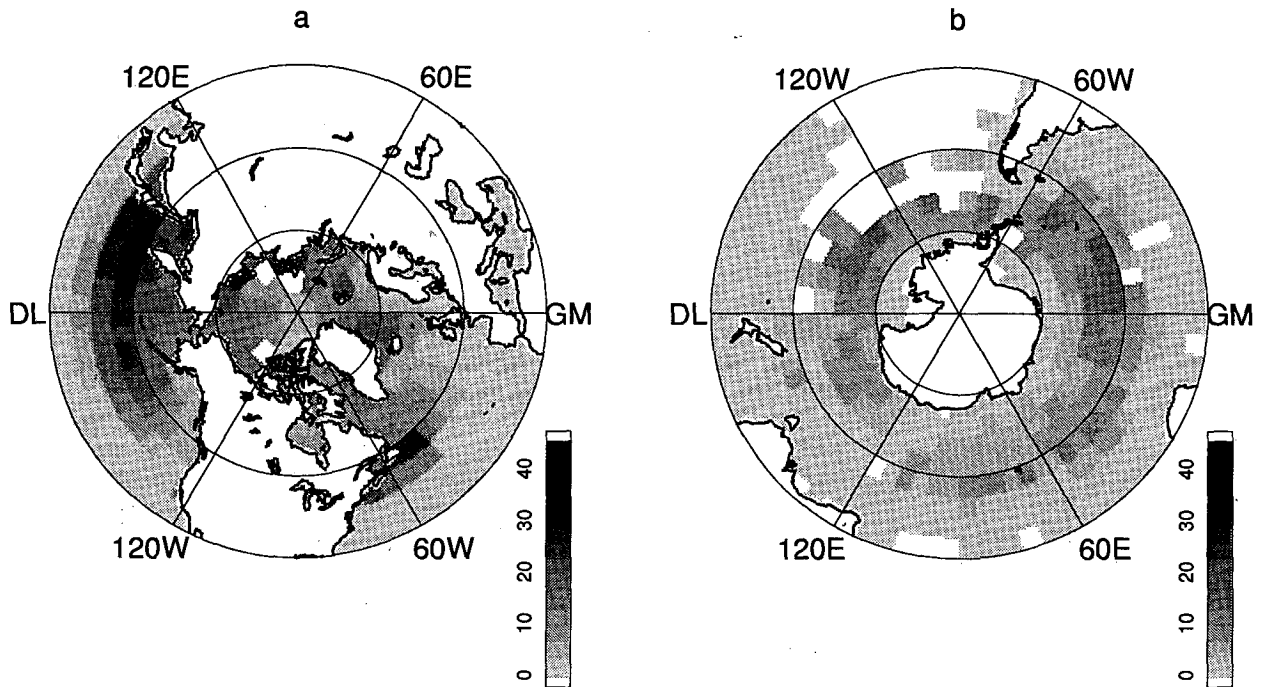


FIG. 11. The frequency of occurrence of sky-obscuring fog in percent for (a) June, July, and August in the Northern Hemisphere, and for (b) December, January, and February in the Southern Hemisphere.

#### d. Arctic stratus

Stratus in the Arctic basin peaks during JJA at nearly 62%, while during the winter season stratus accounts for only 18% cloud cover (Fig. 4d). Herman and Goody (1976) have suggested that the strong seasonal cycle is tied to the annual cycle of temperature in the Arctic basin, whereby the cold winter temperatures of  $-30^{\circ}\text{C}$  prevent the substantial evaporation of moisture from the ice surface. The lack of moisture may explain why this region is the only one of the ten regions in Table 1 where the month of greatest lower-troposphere stability does not coincide with the season of greatest stratus cloud amount.

The importance of advection for Arctic summer stratus has been noted by several authors (Curry et al. 1988; Herman and Goody 1976; Tsay and Jayaweera 1984). The original model of Herman and Goody (1976) conceived of stratus clouds resulting from the influx of warm air from subpolar latitudes into the Arctic basin. With substantial radiative cooling to space and eddy diffusion of heat to the melting ocean or ice pack, the air cools to saturation. Tsay and Jayaweera (1984) noted that clouds in the Beaufort Sea that form in this situation tend to layer and have relatively low cloud bases. Stratus clouds also form from the advection of cold ice pack air over open water, but these clouds tended to have higher cloud bases without layering. Furthermore, they noted that stratus clouds were also associated with occluded fronts that approach from

the Bering Sea. The importance of advection and moisture availability to the occurrence of fog is suggested by the fact that summertime values of fog are greatest on the perimeter of the Arctic Basin where sea ice is a minimum (Fig. 11a).

#### e. Chinese stratus

Stratus in the southeast Chinese plain is very common during the winter and early spring season, with stratus cloud amounts near 50% during DJF and MAM (Fig. 4d). Interestingly, the lower-tropospheric stability [with the ECMWF climatological 1000-mb temperature taken as the lower-level potential temperature in (1)] peaks in February at nearly  $19^{\circ}\text{C}$  and reaches its minimum value in August at  $14^{\circ}\text{C}$ , during the season of the minimum stratus clouds. Apparently this stratus region, like all of those we have studied, is associated with high values of lower-troposphere stability.

What enhances the stability during DJF? Based upon an analysis of FGGE data for the wintertime mean circulation, Murakami (1981) has suggested that a local Hadley circulation develops in the wintertime with rising motion over Malaysia and Indonesia (regions of active wintertime convection) and sinking motion over the surface high pressure that extends southward from Siberia to China. His wintertime 700-mb mean velocity potential has a maximum (indicating the region of strongest divergent outflow) at  $27^{\circ}\text{N}$ ,  $104^{\circ}\text{E}$ , very close to the Warren et al. box with the greatest wintertime

stratus amount ( $25^{\circ}$ – $30^{\circ}$ N,  $105^{\circ}$ – $110^{\circ}$ E, with DJF stratus values of 65%). It is plausible that the sinking motion of air at 700 mb coupled with a good source of low-level moisture leads to the production of stratus clouds and a temperature inversion in the lower atmosphere. During JJA, the monsoon season, mean surface winds are southerly off the South China Sea. These moist southerlies converge at around  $2 \times 10^{-6} \text{ s}^{-1}$ , triggering deep convection rather than shallow stratus clouds.

## 6. Interregional and interannual variations in subtropical marine stratus

While discussing subtropical marine stratus climatologies, it was noted that the seasonal cycle of stratus clouds closely parallels that of the inferred inversion strength, or lower-troposphere stability. Are interregional differences in cloud amounts related to interregional differences in static stability? A scatterplot of seasonally averaged stratus cloud amounts against seasonally averaged static stabilities (1) for each of the five subtropical marine stratus regions and the Chinese stratus region (for a total of 24 points) reveals that to within the uncertainty in the observations ( $1^{\circ}\text{C}$  for stability, 3% for cloud amounts), stratus cloud amounts are very strongly correlated with inferred inversion strengths (Fig. 13). A single linear relationship applies for seasonal variations within individual regions (i.e., stratus clouds occur most during the season of strongest stability), and for interregional variations (i.e., the lower stratus amounts in the Canary Island and Australian regions are associated with values of stability less than  $18^{\circ}\text{C}$ ). The least-squares fit (which explains nearly 90% of the variance) indicates that stratus cloud amounts increase about 6% per  $^{\circ}\text{C}$  increase in the static stability. The association between climatological cloud amounts and inferred inversion strengths is also supported by some observational data from the *Meteor Expedition* of 1925–1927 in the Atlantic (von Ficker 1936a; von Ficker 1936b) [maps reproduced in Hastenrath (1991, pp. 145–149)]. Maps of the temperature increase from the bottom to the top of the trade inversion show that in the Namibian stratus region, where stratus cloud amounts in the annual average are nearly 60%, the typical jump in temperature across the inversion is about  $7^{\circ}\text{C}$  (for the box defined in Table 1), whereas in the Canarian region, where stratus cloud amounts annually average to 23%, the jump in temperature across the inversion is only about  $4^{\circ}\text{C}$ . Data from the cruises of Neiburger et al. (1961) [maps reproduced in Hastenrath (1991), pp. 151–154] show that in the Californian stratus region mean temperature jumps across the inversion are about  $7^{\circ}\text{C}$  during the period June through September.

Also plotted on Fig. 13 are the summertime values of stratus cloud amounts and inversion strengths for the North Pacific and the North Atlantic. In these re-

gions, as discussed above, stratus clouds likely arise from a variety of circumstances (e.g., synoptic events, warm air advection) and in a variety of forms. For example, fog is less dependent on temperature inversions and more dependent on lateral temperature advection. Removing the large component of fog from the stratus cloud amount would bring these points closer to the regression line.

The JJA climatological distribution of stability (Fig. 14) closely matches that of the stratiform cloud climatology for the same season (Fig. 2b). All regions with stability greater than 18 K are regions with high values of low stratiform cloudiness.

With relatively good correspondence between seasonal climatological values of inversion strength and stratus cloud amounts, it would be interesting to look at interannual variations. Fortunately, relatively good climatologies of upper-air and surface-air properties were made at a dozen or so weather ships, mostly in the North Atlantic or North Pacific (Diaz et al. 1987). Figure 15 shows the anomalies during the month of July in total cloud amount and stability (1) from 1950 through 1973 at station N ( $30^{\circ}$ N,  $140^{\circ}$ W, slightly west of the Californian stratus region). Years of high cloud amount generally correspond to years of high stability. From these interannual variations it appears that cloud amounts increase roughly 4% per  $^{\circ}\text{C}$  of stability. It is interesting to note that while 61% of the variance in cloud amount is explained by the stability, only 39% is explained by variations in surface air temperature (and thus SST) (variations in 700-mb temperature explain 28% of the variance in cloud amount). This demonstrates again that anomalies in stratus cloud amount are better related to anomalies in stability than anomalies in surface temperature. Furthermore, anomalies in 700-mb temperature are not a function of anomalies of surface air temperature as 10 of the 21 Julys shown in Fig. 15 had surface air and 700-mb temperature anomalies of opposite sign and 11 Julys had anomalies of the same sign. The trade inversion prevents anomalies in surface temperature from determining anomalies in air temperature above the inversion.

Apart from a few weather ships, the lack of upper-air temperature records only permits us to infer the variations in stability due to the variations in SST alone. The region between  $0^{\circ}$ S and  $10^{\circ}$ S and  $80^{\circ}$ W and  $100^{\circ}$ W, along the coast of South America, is well known as a region of SST interannual variability associated with El Niño. In this region, for the JJA season, stratus cloud amounts for the years 1952–1981 are negatively correlated with SSTs, with a correlation coefficient of  $-0.76$  (Fig. 16). The four years with the lowest amounts of stratus (less than 40% when typical values are nearly 55%) occurred during the years of warmest SSTs ( $\text{SST} > 23^{\circ}\text{C}$ ); these four years, 1957, 1965, 1972, and 1976, were El Niño years (Rasmusson and Carpenter 1982). A least-squares fit indicates a

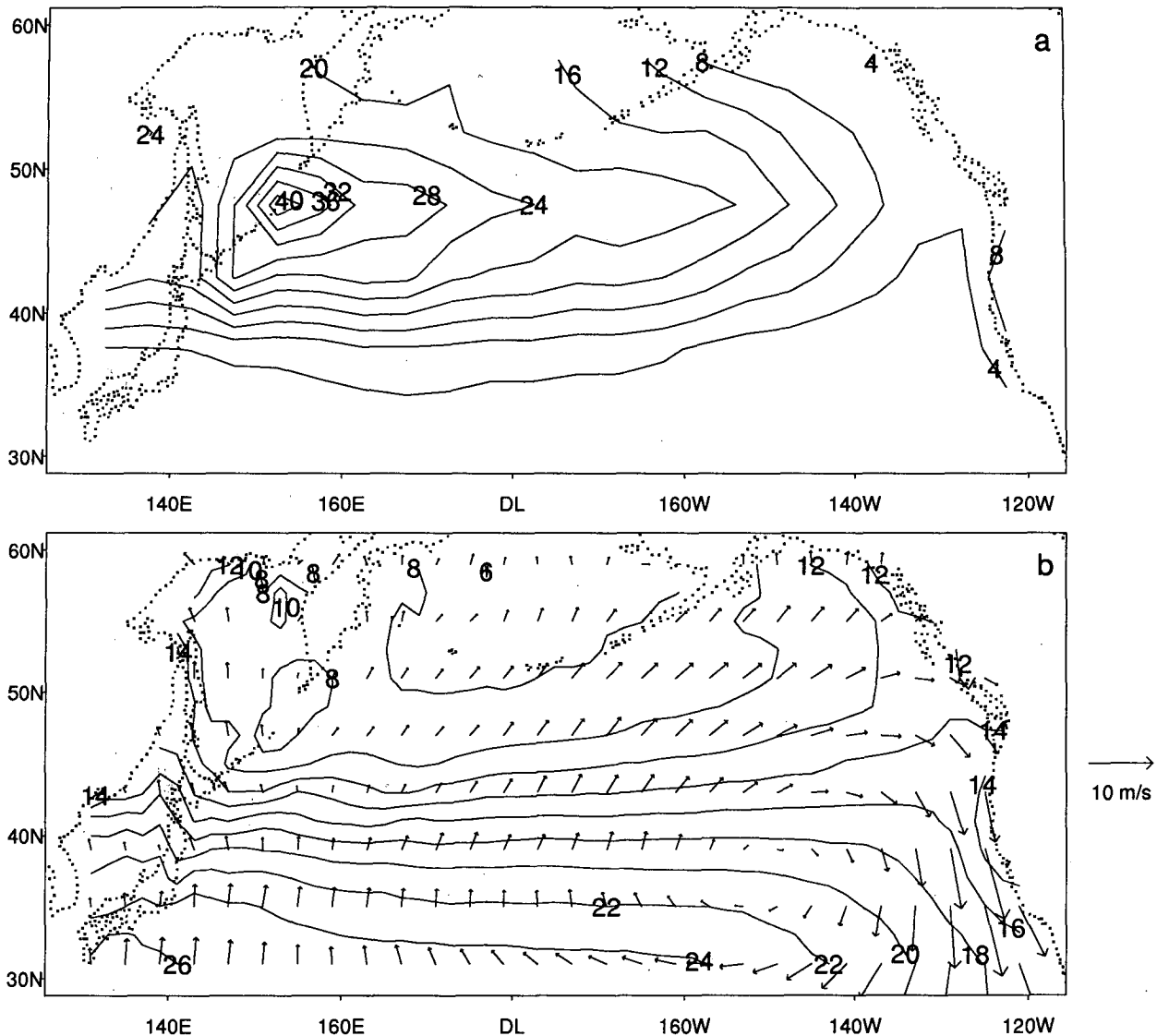


FIG. 12. (a) The frequency of sky-obscuring fog in June, July, and August in the North Pacific (contour interval is 4%); (b) the sea surface temperature and mean (smoothed) surface winds for the same region and season (contour interval is 2°C); (c) the frequency of sky-obscuring fog in June, July, and August in the North Atlantic (contour interval is 4%); and (d) the sea surface temperature and mean (smoothed) surface winds for the same region and season (contour interval is 2°C).

decrease of stratus cloudiness of about 5% per °C, which agrees with the increases of 6% cloudiness per °C of stability inferred from Fig. 13. If data were available for air temperatures above the inversion in this region, we would expect to get a better relationship between stratus cloud amount and static stability than with sea surface temperature alone. Deser and Wallace (1990) also found that in this region total cloudiness decreases 0.5 okta (6.25%) per °C increase in their equatorial SST index. Hanson (1991) has shown that variations in total cloud amount are weakly correlated with variations in SSTs for the subtropical Atlantic and Pacific stratus regions. He estimated a lower sensitivity of total cloud amount to SST, roughly 1.5% per °C.

## 7. Discussion

What is the physical meaning of the association between stratus clouds and inferred inversion strengths? It is believed that with a temperature inversion at the top of the boundary layer, moisture that is evaporated from the sea surface will accumulate and gradually reach saturation. Once a cloud has been formed, convection is easily maintained, primarily due to the strong radiative cooling at cloud top (which occurs in the absence of other clouds above). This stratus cloud is confined to the boundary layer because cloudy eddies are unable to penetrate the inversion. It would appear that for stratus clouds to exist, an inversion must be present.

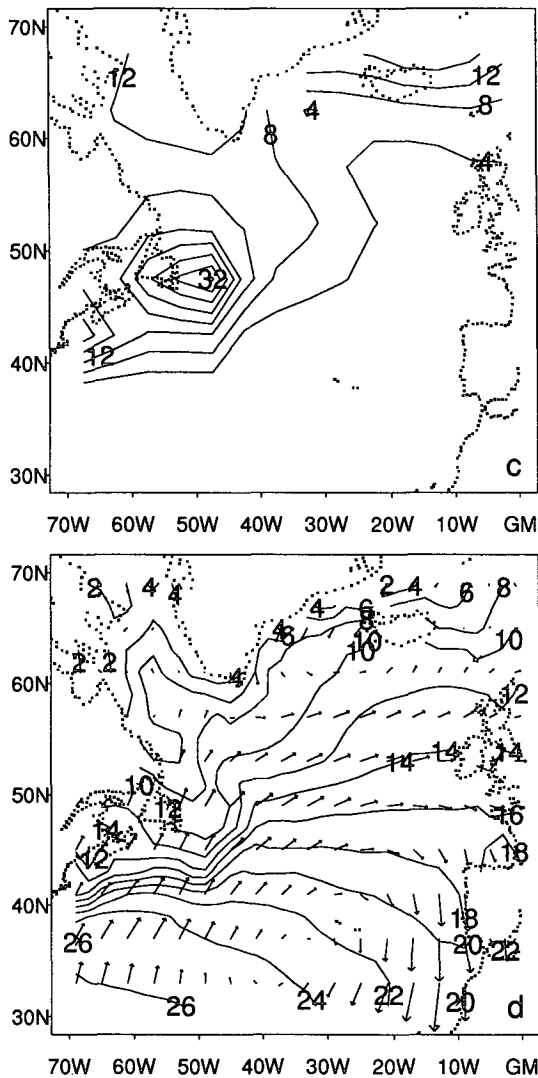


FIG. 12. (Continued)

But because little theory exists to explain what controls the fractional cloudiness of stratus, there is no a priori reason for why changes in the strength of the inversion should be associated with changes in cloud amount.

Previous studies of stratus cloud amount have focused on whether or not the cloud top is stable to entrainment; this potential instability of the cloud top to mixing with air from above the inversion has been termed cloud-top entrainment instability (CTEI) (Deardorff 1980; Randall 1980). However, Albrecht's study (1991) of individual soundings from the Atlantic Tradewind Experiment (ATEX) showed that cloud amounts were not correlated with the thermodynamic criterion for CTEI or the mixing line slope that Betts and Boers (1990) had proposed as a measure of stratus cloud amount. Thus, previous attempts to parameterize stratus amounts by considering daily variations at a

single location (and not seasonal and interannual variations over large regions, as we have done) have been unsuccessful.

The connection between subtropical stratus clouds and static stability suggests the possibility of a positive feedback (Hanson 1991). Stratus clouds help keep the boundary layer relatively cool through the longwave cooling at cloud top and the reflection of shortwave energy back to space. If the amount of stratus is sensitive to the static stability, then the cooling of boundary-layer air by the clouds may help to increase the static stability and thus potentially the cloud amount. Boundary-layer air temperatures are in large part determined by the SSTs. However, due to the greater heat capacity of the ocean, the SSTs themselves may be relatively insensitive to the radiation changes. This would limit the effectiveness of such feedback. Of course, it must be stressed that the association between static stability and stratus clouds does not necessarily imply a causal relationship (*in either direction*).

The connection between subtropical stratus clouds and lower-tropospheric stability has been employed in the ECMWF parameterization of low clouds of the subtropical stratus type (Slingo 1980; Slingo 1987). In this scheme, if an inversion is found beneath 700 mb, then the low-cloud amount is parameterized as proportional to the lapse rate in the most stable layer. The potential for a positive feedback in this scheme was

Stratus Cloud Amount vs. Stability

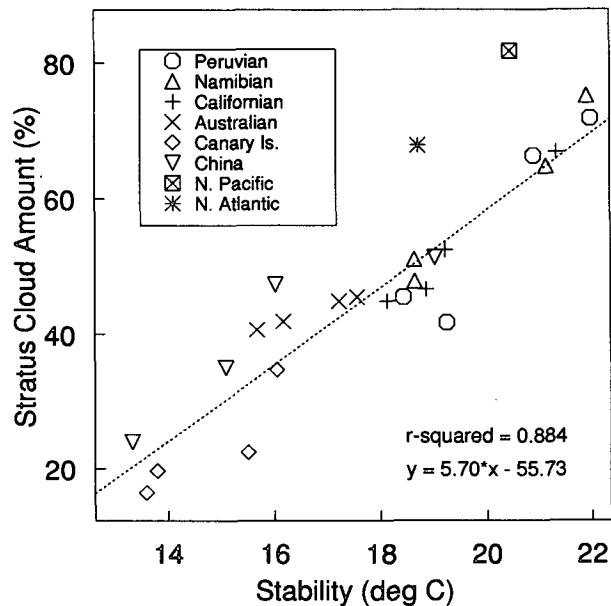


FIG. 13. Scatterplot of seasonally averaged stratocumulus cloud amount with seasonally averaged lower-tropospheric stability for the five subtropical oceanic regions and the Chinese stratus region. In addition, the June, July, and August seasonally averaged quantities are plotted for the North Pacific and North Atlantic but are not included in the regression.

### JJA Stability

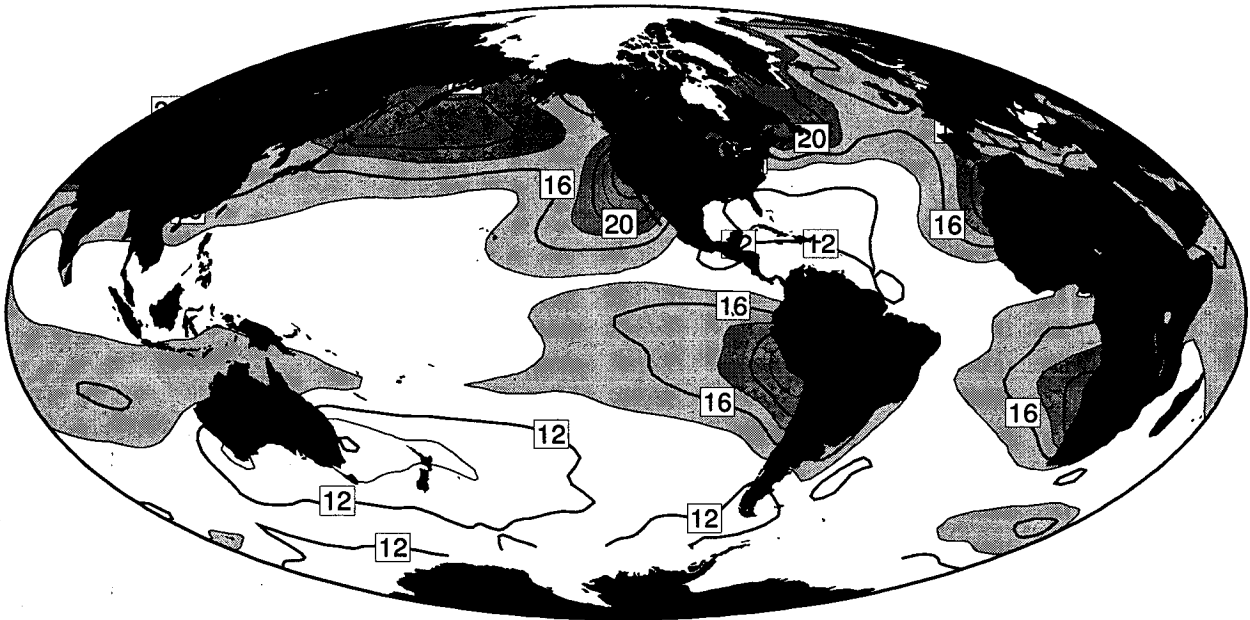


FIG. 14. Climatological values of lower-tropospheric static stability for the June, July, and August season in degrees Celsius. Contour interval is 2°C.

noted, as the low cloud amount from a five-day forecast was significantly greater for the forecast where the radiation changes associated with the clouds could affect the stability and the cloud amount than for the forecast with this interaction shut off (Slingo 1987). In a GCM with simplified boundary-layer physics, the absence of turbulent mixing processes in the boundary layer (such

as entrainment warming) that could compensate for the radiative cooling permitted the feedback to be quite strong. This parameterization of low cloud amount based on stability has recently been incorporated in

Cloud Amount vs. Stability Anomalies, July, Station N

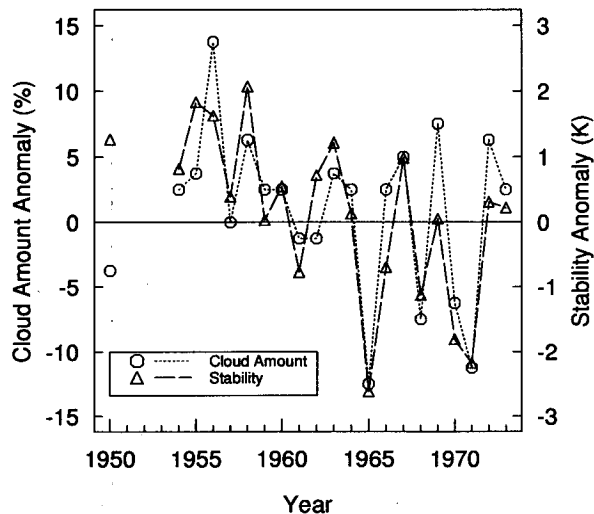


FIG. 15. Time series of the July anomalies in total cloud amount and lower-tropospheric stability at weather ship N (30°N, 140°W).

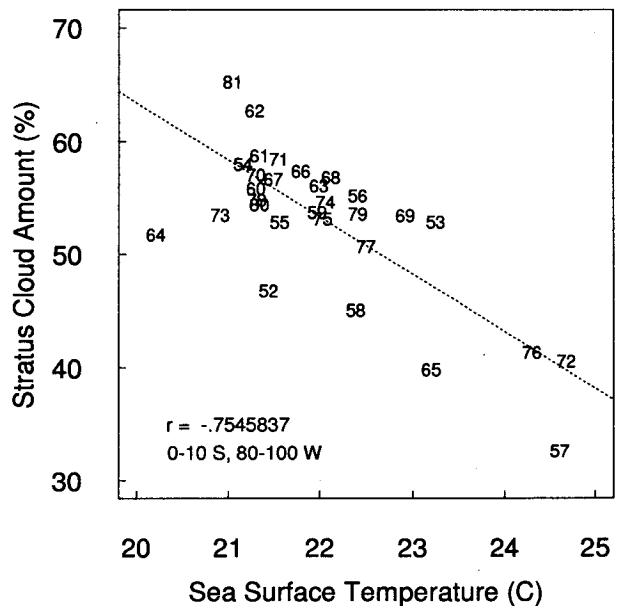


FIG. 16. Scatterplot of the average sea surface temperature and stratus cloud amount for the June, July, and August season for the 1952–1981 time period for the region 0°–10°S, 80°–100°W. Numbers plotted indicate the year (minus 1900) of the data. The line plotted is a least-squares fit.

the NCAR Community Climate Model (CCM) (Slingo and Slingo 1991).

## 8. Summary

In this paper, the seasonal distribution of low stratiform cloudiness has been explored with the aim of understanding the factors responsible for the presence of these clouds. Through experimental programs such as ERBE, these clouds have been shown to strongly impact the net radiation balance. Being more reflective than the underlying surface, they substantially increase the planetary albedo. Because these clouds are low, they generally do not strongly affect the amount of thermal radiation escaping to space. The combination of these two effects makes the radiation balance of the planet strongly sensitive to changes in the abundance of these clouds (or to other cloud properties such as effective cloud-drop radius or liquid water path).

Using a surface-based climatology of stratus clouds, ten regions of climatologically high values of stratus clouds have been defined. With the exception of wintertime stratus in the southeast Chinese plain, the regions of greatest stratus all occur over the oceans. These ten regions fall into a few classes: subtropical marine stratus, midlatitude oceanic stratus, Arctic stratus, and Chinese stratus. In all stratus regions (except the Arctic), the season of greatest stratus cloud amount coincides with the season of greatest lower-tropospheric stability. This reflects the preference of stratus to form under a well-defined inversion. In the subtropics, stratus forms beneath the well-known trade inversion that presumably results from subsidence in the descending branch of the Hadley Cell. Midlatitude oceanic stratus occurs in all seasons with cloud amounts greater than 50%, with the most stratus occurring during the summer season. The midlatitude summertime inversions likely result from subsidence in the descending branches of monsoonlike circulations between the much warmer continents and the colder ocean. Midlatitude stratus clouds have a very strong impact on the net radiation budget with summertime values of cloud forcing lower than  $-100 \text{ W m}^{-2}$ .

For the subtropical and Chinese stratus regions a single linear relationship between static stability and cloud amount appears to explain the seasonal, interregional, and interannual variations. The slope of this regression line indicates that the stratus clouds increase their area coverage by 6% per degree increase in static stability. These clouds appear to be sensitive to changes in lower-troposphere stability and not surface temperature alone. Thus, the response of low stratiform clouds to a climate change cannot be determined from the change in surface temperature alone but requires consideration of the vertical structure of temperature in the lower troposphere.

Over midlatitude oceans, sky-obscuring fog is a large fraction of the summertime stratus cloud amount as

reported in the Warren et al. atlases (1986, 1988). Because fog is sensitive to horizontal temperature advection, the climatological values of stratus (which include a large fog component) did not fall close to the regression line indicated by the stability-stratus cloud amount relationship in the subtropical and Chinese regions. In the Arctic, the abundance of moisture (which is related to the annual temperature cycle) appears to determine the annual cycle of stratus rather than the stability.

The amounts of stratus clouds appear to be closely tied to aspects of the general circulation of the atmosphere and ocean. The inversion at the top of the boundary layer appears to play a central role in the existence of stratus. The strength of the subtropical trade inversion, which is observed to be related to the amount of stratus, is tied to the strength of the Hadley Cell, which in turn is partly determined by the amount of deep convection taking place in the tropics. Monsoonlike circulations between the midlatitude continents and oceans may strengthen in a global warming scenario in which the continents warm faster than the oceans, which would lead to the production of more midlatitude summertime oceanic stratus. This would (by the reflection of more sunlight) strengthen the ocean-land surface temperature difference and further intensify the strength of the monsoonlike circulation. Fog over the midlatitude oceans is related to the predominant southerly flow down a steep gradient in SSTs. Advection of air masses in the Arctic play a role in determining the abundance of stratus. All of these interactions between low stratiform clouds and the general circulation of the atmosphere and ocean make predicting their response to climate change a complex problem.

*Acknowledgments.* This work was supported by NASA EOS Grant NAGW-2633 and in part by an ERBE grant, Contract NAS1-18157. Stephen A. Klein is supported by a NASA Global Change Fellowship, NASA Grant NGT-30033. The authors also wish to thank Chris Bretherton, Conway Leovy, and Marcia Baker for their helpful discussions, and Marc Michelsen for assistance with the computations.

## REFERENCES

- Albrecht, B. A., 1991: Fractional cloudiness and cloud-top entrainment instability. *J. Atmos. Sci.*, **48**, 1519–1525.
- , D. A. Randall, and S. Nicholls, 1988: Observations of marine stratocumulus during FIRE. *Bull. Amer. Meteor. Soc.*, **69**, 618–626.
- Barkstrom, B. R., 1984: The Earth Radiation Budget Experiment. *Bull. Amer. Meteor. Soc.*, **65**, 1170–1185.
- , and G. L. Smith, 1986: The Earth Radiation Budget Experiment: Science and implications. *Rev. Geophys.*, **24**, 379–390.
- Betts, A. K., and R. Boers, 1990: A cloudiness transition in a marine boundary layer. *J. Atmos. Sci.*, **47**, 1480–1497.
- Bond, N. A., 1992: Observations of planetary boundary-layer structure in the eastern equatorial Pacific. *J. Climate*, **5**, 699–706.
- Cess, R. D., and Collaborators, 1989: Interpretation of cloud-climate

- feedback as produced by 14 atmospheric general circulation models. *Science*, **245**, 513–516.
- Curry, J. A., E. E. Ebert, and G. F. Herman, 1988: Mean and turbulence structure of the summertime Arctic cloud boundary layer. *Quart. J. Roy. Meteor. Soc.*, **114**, 715–746.
- Deardorff, J. W., 1980: Cloud top entrainment instability. *J. Atmos. Sci.*, **37**, 131–147.
- Deser, C., and J. M. Wallace, 1990: Large-scale atmospheric circulation features of warm and cold episodes in the tropical Pacific. *J. Climate*, **3**, 1254–1281.
- Diaz, H. F., C. S. Ramage, S. D. Woodruff, and T. S. Parker, 1987: *Climatic Summaries of Ocean Weather Stations*. National Oceanic and Atmospheric Administration, Environmental Research Laboratories, Air Resources Laboratory, Climate Research Division, Boulder, CO, 49 pp.
- Hanson, H. P., 1991: Marine stratocumulus climatologies. *Int. J. Clim.*, **11**, 147–164.
- Harrison, E. F., P. Minnis, B. R. Barkstrom, V. Ramanathan, R. D. Cess, and G. G. Gibson, 1990: Seasonal variation of cloud radiative forcing derived from the Earth Radiation Budget Experiment. *J. Geophys. Res.*, **95**, 18 687–18 703.
- Hartmann, D. L., M. E. Ockert-Bell, and M. L. Michelsen, 1992: The effect of cloud type on earth's energy balance: Global analysis. *J. Climate*, **5**, 1281–1304.
- Hastenrath, S., 1991: *Climate Dynamics of the Tropics*, updated edition, Kluwer Academic Publishers, 488 pp.
- Herman, G., and R. Goody, 1976: Formation and persistence of summertime arctic stratus clouds. *J. Atmos. Sci.*, **33**, 1537–1553.
- Lilly, D. K., 1968: Models of cloud-topped mixed layers under a strong inversion. *Quart. J. Roy. Meteor. Soc.*, **94**, 292–309.
- Manabe, S., and R. F. Strickler, 1964: Thermal equilibrium of the atmosphere with a convective adjustment. *J. Atmos. Sci.*, **21**, 361–385.
- , and R. T. Wetherald, 1967: Thermal equilibrium of the atmosphere with a given distribution of relative humidity. *J. Atmos. Sci.*, **24**, 241–259.
- Moeng, C.-H., 1986: Large-eddy simulation of a stratus-topped boundary layer. Part I: Structure and budgets. *J. Atmos. Sci.*, **43**, 2886–2900.
- Murakami, T., 1981: Orographic influence of the Tibetan plateau on the Asiatic winter monsoon circulation. Part I. Large-scale aspects. *J. Meteor. Soc. Japan*, **59**, 40–65.
- Neiburger, M., D. S. Johnson, and C. W. Chien, 1961: *Studies of the Structure of the Atmosphere over the Eastern Pacific Ocean. I: The Inversion over the Eastern North Pacific ocean*. University of California Press, 94 pp.
- Ramanathan, V., R. D. Cess, E. F. Harrison, P. Minnis, B. R. Barkstrom, E. Ahmad, and D. L. Hartmann, 1989: Cloud-radiative forcing and climate: Results from the Earth Radiation Budget Experiment. *Science*, **243**, 57–63.
- Randall, D. A., 1980: Conditional instability of the first kind upside-down. *J. Atmos. Sci.*, **37**, 125–130.
- , J. A. Abeles, and T. G. Corsetti, 1985: Seasonal simulations of the planetary boundary layer and boundary-layer stratocumulus with a general circulation model. *J. Atmos. Sci.*, **42**, 641–676.
- , J. A. Coakley Jr., C. W. Fairall, R. A. Kropfli, and D. H. Lenschow, 1984: Outlook for research on subtropical marine stratiform clouds. *Bull. Amer. Meteor. Soc.*, **65**, 1290–1301.
- Rasmusson, E. M., and T. H. Carpenter, 1982: Variations in tropical sea surface temperature and surface wind fields associated with the Southern Oscillation/El Niño. *Mon. Wea. Rev.*, **110**, 354–384.
- Riehl, H., T. C. Yeh, J. S. Malkus, and N. E. LaSeur, 1951: The north-east trade of the Pacific ocean. *Quart. J. Roy. Meteor. Soc.*, **77**, 598–626.
- Rosow, W. B., and R. A. Schiffer, 1991: International Satellite Cloud Climatology Project (ISCCP) cloud data products. *Bull. Amer. Meteor. Soc.*, **72**, 2–20.
- Schubert, W. H., J. S. Wakefield, E. J. Steiner, and S. K. Cox, 1979a: Marine stratocumulus convection. Part I: Governing equations and horizontally homogeneous solutions. *J. Atmos. Sci.*, **36**, 1286–1307.
- , —, —, and —, 1979b: Marine stratocumulus convection. Part II: Horizontally inhomogeneous solutions. *J. Atmos. Sci.*, **36**, 1308–1324.
- Slingo, A., 1990: Sensitivity of the earth's radiation budget to changes in low clouds. *Nature*, **343**, 49–51.
- , and J. M. Slingo, 1991: Response of the National Center for Atmospheric Research community climate model to improvements in the representation of clouds. *J. Geophys. Res.*, **96**, 15 341–15 357.
- Slingo, J. M., 1980: A cloud parametrization scheme derived from GATE data for use with a numerical model. *Quart. J. Roy. Meteor. Soc.*, **106**, 747–770.
- , 1987: The development and verification of a cloud prediction scheme for the ECMWF model. *Quart. J. Roy. Meteor. Soc.*, **113**, 899–927.
- Tsay, S., and K. Jayaweera, 1984: Physical characteristics of Arctic stratus clouds. *J. Climate Appl. Meteor.*, **23**, 584–596.
- Von Ficker, H., 1936a: Bemerkungen über den Wärmeumsatz innerhalb der Passatzirkulation. *Sitzungsberichte der Preussischen Akademie der Wissenschaften Phys. Math. Klasse*, **11**, 102–114.
- , 1936b: *Die Passatinversion*. Veröffentlichungen Meteorol. Institut, Universität Berlin, 33 pp.
- Warren, S. G., C. J. Hahn, J. London, R. M. Chervin, and R. L. Jenne, 1986: Global distribution of total cloud cover and cloud type amounts over land. NCAR Tech. Note NCAR/TN-273+STR, National Center for Atmospheric Research, Boulder, CO, 29 pp. plus 200 maps.
- , —, —, —, and —, 1988: Global distribution of total cloud cover and cloud type amounts over ocean. NCAR Tech. Note NCAR/TN-317+STR, National Center for Atmospheric Research, Boulder, CO, 42 pp. plus 170 maps.
- Woodruff, S. D., R. J. Slutz, R. L. Jenne, and P. M. Steurer, 1987: A Comprehensive Ocean-Atmosphere Data Set. *Bull. Amer. Meteor. Soc.*, **68**, 1239–1250.
- World Meteorological Organization, 1974: *Manual on Codes*, Vol. 1. WMO Publication No. 306, World Meteorological Organization, Geneva, 328 pp.